bioRxiv preprint doi: https://doi.org/10.1101/2022.06.17.496647; this version posted June 20, 2022. The copyright holder for this preprint (which was not certified by peer review) is the author/funder, who has granted bioRxiv a license to display the preprint in perpetuity. It is made available under aCC-BY-NC-ND 4.0 International license.

Human concurrent intracranial EEG and fMRI reveals multiple temporally independent but spatially similar connectome trajectories across timescales

Parham Mostame[1,2,*], Jonathan Wirsich[3], Thomas H. Alderson[1,2], Ben Ridley[4,5], David Carmichael[6,7], Serge Vulliemoz[3], Maxime Guye[4,8], Louis Lemieux[9,10], Sepideh Sadaghiani[1,2]

[1] Department of psychology, University of Illinois at Urbana-Champaign, Champaign, IL, USA

[2] Beckman Institute for Advanced Science and Technology, University of Illinois at Urbana-Champaign, Champaign, IL, USA

[3] EEG and Epilepsy Unit, University Hospitals and Faculty of Medicine of Geneva, University of Geneva, Geneva, Switzerland

[4] Aix Marseille Univ, CNRS, CRMBM, France

[5] IRCCS Istituto delle Scienze Neurologiche di Bologna, Bologna, Italy

[6] Developmental Imaging and Biophysics Section, UCL Great Ormond Street Institute of Child Health, London, United Kingdom

[7] Wellcome EPSRC Centre for Medical Engineering, King's College London, St Thomas' Hospital, London, United Kingdom

[8] AP-HM, Hôpital Universitaire Timone, Pôle d'Imagerie Médicale, CEMEREM, Marseille, France

[9] Department of Clinical and Experimental Epilepsy, UCL Queen Square Institute of Neurology, London, UK

[10] Epilepsy Society MRI Unit, Chalfont St Peter, Buckinghamshire, UK

* Corresponding Author (mostame2@illinois.edu)

Abstract

The large-scale organization of functional connectivity (FC) — the functional connectome — traverses distinct spatial patterns in a dynamic trajectory as demonstrated independently in fMRI and electrophysiological studies. These patterns are thought to satisfy ever-changing processing demands. FMRI and electrophysiology capture partly non-overlapping neural populations at different timescales, and it remains unknown to what degree the dynamic connectome trajectories across the two modalities are associated. We sought to clarify this relationship by studying resting wakefulness in a rare concurrent intracranial EEG and functional MRI dataset (iEEG-fMRI; 9 human neurosurgical patients) and in whole-brain connectomes obtained from source-localized EEG-fMRI (26 healthy humans). We measured "spatial convergence" as cross-modal spatial similarity of connectome configurations at a given time, and "temporal convergence" as synchronous occurrence of spatial convergence. We investigated three possible scenarios characterizing the cross-modal association of connectome trajectories: I) spatially and temporally convergent, II) spatially convergent but temporally divergent, and III) spatially and temporally divergent. We found that the behavior of fMRI and iEEG/EEG is consistent with scenario II: connectome trajectories spatially converge at intermittent times. Importantly, such asynchronous spatial convergence of connectome configurations was driven by cross-modally matched recurrent connectome states, independently across electrophysiological timescales. This connectome-level multi-frequency spatial convergence and temporal divergence suggests that hemodynamic and electrophysiological signals capture distinct aspects of FC, rather than serving as intermodal measurements of the same phenomenon. The multitude of flexible trajectories across timescales may concurrently enable FC across multiple independent sets of distributed brain regions.

bioRxiv preprint doi: https://doi.org/10.1101/2022.06.17.496647; this version posted June 20, 2022. The copyright holder for this preprint (which was not certified by peer review) is the author/funder, who has granted bioRxiv a license to display the preprint in perpetuity. It is made available under aCC-BY-NC-ND 4.0 International license.

Introduction

The traditional view that functional connectivity (FC) primarily emerges in response to cognitive demands has been giving way to more recent observations that FC is predominantly intrinsic in nature (Gratton et al., 2018; Mostame and Sadaghiani, 2020a). The functional connectome, which constitutes the whole-brain spatial organization of large-scale FC, continuously exhibits *reconfigurations* across different spatial patterns in all mental states including task-free rest. These reconfigurations are referred to as spontaneous or ongoing FC dynamics (Preti et al., 2017; Lurie et al., 2018; Sadaghiani and Wirsich, 2019). Such ongoing FC dynamics in both fMRI and electrophysiology affect cognitive functions and the processing of external stimuli (Weisz et al., 2014; Sadaghiani and D'Esposito, 2015; Cohen, 2018; Rassi et al., 2019). More specifically, spontaneously occurring FC configurations are thought to represent distinct discrete connectome states that support different cognitive processes; Thus, iteration through these states may be commensurate with maintaining cognitive flexibility during all cognitive states including rest (Deco et al., 2013; Vohryzek et al., 2020).

While the functional connectome is commonly studied with fMRI, a growing body of work suggests that it can be reliably observed using electrophysiological methods such as MEG, EEG, and intracranial EEG (iEEG) (Sadaghiani and Wirsich, 2019; Sadaghiani et al., 2021). FC captured in fMRI and electrophysiology is partly distinct with respect to the underlying neural populations, connectivity mechanisms, and timescales. Specifically, while the Local Field Potential signal of electrophysiological methods including intracranial recordings is dominated by pyramidal neurons (Buzsáki et al., 2012), the fMRI signal stems from the metabolic demands of neural activity that can cumulatively reflect a large variety of neural populations (Heeger and Ress, 2002). Extending this notion to timescales, Hari and Parkkonen (2015) argue that neural ensembles connected via slow (thin, unmyelinated) fibers are more prominent in the fMRI signal, while neural activity involving fast-conducting (thick, myelinated) fibers is better captured in electrophysiological data. Regarding FC in particular, fMRI and electrophysiological recordings differ in terms of both speed and connectivity mechanisms; fMRI captures connectivity based on slow co-fluctuations of the hemodynamic signal thus resulting in connectome dynamics in the range of seconds to minutes (Chang and Glover, 2010; Calhoun et al., 2014; Vohryzek et al., 2020). Conversely, connectivity in electrophysiology commonly reflects cross-region coupling of phase or amplitude of fast neural oscillations (~1-150 Hz), resulting in connectome dynamics at sub-second speeds (Baker et al., 2014; Hunyadi et al., 2019). Such oscillation-based coupling mechanism is thought to enable rhythmic frequency-specific modes of rapid neural communication that may represent independent channels of information exchange (Mostame and Sadaghiani, 2020a). Given that the spontaneous reorganization of the connectome is primarily observed in separate fMRI and electrophysiological experiments, a multimodal approach that bridges across largescale FC timescales is indicated. More generally, ultimately all observations of any given phenomenon must be reconciled.

Prior multimodal work has begun to directly investigate the relationship between hemodynamics- and electrophysiology-derived connectomes. The *time-averaged (static)* spatial organization of functional

bioRxiv preprint doi: https://doi.org/10.1101/2022.06.17.496647; this version posted June 20, 2022. The copyright holder for this preprint (which was not certified by peer review) is the author/funder, who has granted bioRxiv a license to display the preprint in perpetuity. It is made available under aCC-BY-NC-ND 4.0 International license.

connectomes is correlated between fMRI and electrophysiological data including MEG (Brookes et al., 2011; Hipp and Siegel, 2015), EEG (Deligianni et al., 2014; Wirsich et al., 2017), and iEEG (Ridley et al., 2017; Kucyi et al., 2018; Betzel et al., 2019). However, irrespective of electrophysiological modality, only moderate correlation values are reported at the group-level (commonly r = ~0.3) for the various individual electrophysiological frequency bands. Importantly, this moderate effect size has been replicated in several EEG-fMRI datasets differing in hardware, scanning conditions and subject populations (Wirsich et al., 2021). At individual subject level, the spatial similarity is smaller (Hipp and Siegel, 2015; Wirsich et al., 2021). Whether the divergence of static hemodynamics- and electrophysiology-derived connectomes mostly reflects different neurobiological dynamics at different FC timescales or some other factor is unclear.

To answer this question, a handful of studies have recently extended investigations of the cross-modal link between fMRI and electrophysiology to *time-varying* FC changes. We have shown that fMRI connections with stronger FC temporal variance correspond to connections with higher FC variance in intracranial EEG (Ridley et al., 2017). We have further shown that *infraslow* FC dynamics (60s temporal resolution) in fMRI are associated with phase-coupling of concurrent source-localized scalp EEG at the level of individual connections (Wirsich et al., 2020b). For all EEG frequency bands, this cross-modal association was observed in a large set of distributed connections. However, when moving from connection-level FC to large-scale spatial configurations of FC (i.e. *patterns* over all connections), the cross-modal relation of dynamics appears to be temporally sparse. Specifically, investigating such spatial FC patterns at *infraslow* temporal resolution (~40s windows), Abreu and colleagues (2020) report that two of ten connectome configurations observed in fMRI and in concurrent source-localized EEG were spatially correlated, while eight in each modality were unmatched. In other work, Zhang et. al (2020) have shown in rats, that instantaneous patterns of fMRI coactivation with respect to a seed region (i.e. coactivation patterns / "CAPs") are spatially similar when obtained from BOLD or LFP signals of the seed regions. Importantly, this similarity primarily occurs during sparse events (when the seed region signal is at its peak level). In sum, beyond a certain level of *convergence that is robust but limited* (Wirsich et al., 2021), the above-discussed static and time-varying FC studies also demonstrate considerable *divergence* between fMRI and electrophysiological findings (Wirsich et al., 2020a).

One possible explanation for partial spatial and temporal divergence of FC dynamics not commonly considered, is that fMRI and electrophysiological measures each weigh more strongly different neural processes or populations, as discussed above (Nunez and Silberstein, 2000; Hari and Parkkonen, 2015; Hermes et al., 2017). Studying the spatiotemporal relationship of FC dynamics at sub-second temporal resolution can provide insights into this possibility. To understand connectome dynamics across FC timescales, we measure the degree to which fMRI and electrophysiology capture *overlapping* connectivity processes. Figure 1 illustrates three major scenarios of possible convergence/divergence. Specifically, moment-to-moment connectome configurations observed in the two modalities (I) may constitute epochs of spatially similar connectome patterns occurring at the same time (spatially and temporally convergent), or (II), may be driven by largely distinct

bioRxiv preprint doi: https://doi.org/10.1101/2022.06.17.496647; this version posted June 20, 2022. The copyright holder for this preprint (which was not certified by peer review) is the author/funder, who has granted bioRxiv a license to display the preprint in perpetuity. It is made available under aCC-BY-NC-ND 4.0 International license.

temporal trajectories that, however, enact similar connectome patterns (spatially convergent, temporally divergent), and finally (III), may be driven by largely non-overlapping temporal trajectories with spatially non-overlapping connectome patterns (spatially and temporally divergent).

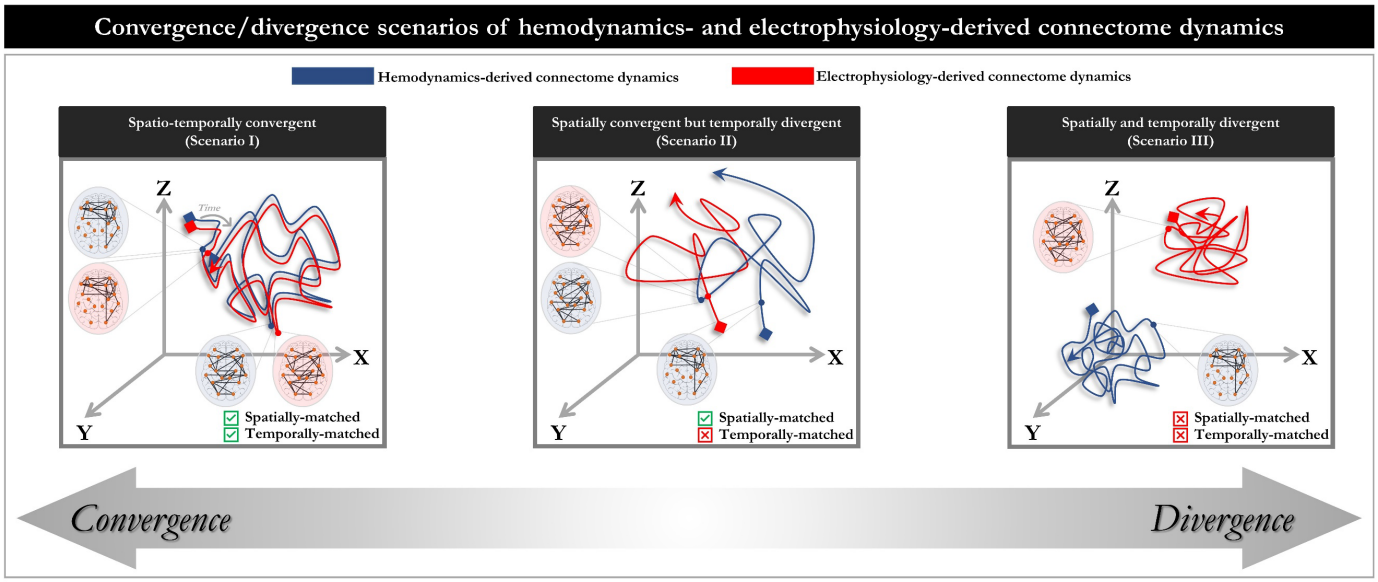

Fig. 1 – ***Three potential scenarios for convergence/divergence of connectome trajectories across hemodynamics and electrophysiology.*** *Dynamics of connectome reconfigurations (i.e. time-varying spatial patterns of large-scale connectivity) are shown as trajectories in a presumed 3D state space, starting from the diamond sign and ending at the arrowhead. Hemodynamics- and electrophysiology-derived connectome dynamics in each scenario are shown in blue and red, respectively. Scenario (I): both dynamic trajectories are driven by the same connectivity processes; are spatially and temporally convergent (at all times). Scenario (II): both dynamic trajectories span the same portion of the state space, while each traversing a different timecourse; are spatially convergent but temporally divergent. Scenario (III): each of the dynamic trajectories span non-overlapping parts of the state space with different timecourses; are spatially and temporally divergent (at all times). Note that scenarios I and III represent border cases extracted from a theoretical convergence/divergence gradient (bottom of the figure). Spatial convergence does not imply a perfect spatial match (at the same or different time points) given established observations that the cross-modal similarity in static connectomes is moderate (Betzel et al., 2019; Wirsich et al., 2021). Further, electrophysiology-derived connectivity may have several trajectories operating in frequency-specific channels.*

We adjudicate the likelihood of these scenarios by comparing connectome configurations across fMRI and concurrent intracranial EEG in *synchronous* (time-aligned comparison of connectomes) and *asynchronous* (a novel, time-shifted comparison of connectomes) analysis approaches. In the so-called resting state, characterized by the absence of experiment control, the brain's activity can be described as spontaneous and therefore *a priori*, each moment can be taken as unique: irreproducible. Therefore, all signals of interest must be recorded simultaneously. The concurrent recording of hemodynamic and electrophysiological brain signals allows us to investigate the direct association of connectome configurations across FC timescales in a frame-by-frame manner (in both synchronous and asynchronous approaches), which is not possible in separately acquired multi-modal datasets. After establishing robust effects intracranially in the absence of volume conduction, we extend our approach to whole-brain (whole-cortex) functional connectomes derived from concurrent fMRI and source-localized EEG recordings of healthy subjects.

bioRxiv preprint doi: https://doi.org/10.1101/2022.06.17.496647; this version posted June 20, 2022. The copyright holder for this preprint (which was not certified by peer review) is the author/funder, who has granted bioRxiv a license to display the preprint in perpetuity. It is made available under aCC-BY-NC-ND 4.0 International license.

Results

This study determines the spatial and temporal convergence across dynamic reconfigurations of FC patterns in hemodynamic and electrophysiological measures. We first focus on a concurrent intracranial EEG (iEEG) and fMRI dataset minimally affected by volume conduction (N = 9; Fig. 2 & 3), we then extend our findings to whole-brain connectomes of healthy subjects using a secondary concurrent *source-localized* scalp EEG and fMRI dataset (N = 26; Fig. 4). Using the source-localized data, we further characterize whole-brain recurrent connectome states underlying the cross-modal convergence (Fig. 5). Intracranial grid and depth electrode locations are shown in Fig. S1. While iEEG FC patterns represent only a partial window of the whole- brain connectome, we use the term "connectome" to refer to both iEEG FC patterns (partial brain window) and EEG FC patterns (whole-brain).

For each subject, we calculated the FC configuration at every 100ms for fMRI (fMRI-FC) and band-limited iEEG amplitude coupling (iEEG-FC_{Amp}), and spatially compared them across modalities. For both datasets, we include replication of results using phase coupling (denoted as iEEG-FC_{Phase}) as a supplemental analysis. Note that the high temporal sampling in fMRI-FC exploited a recently introduced single-volume measure of instantaneous co-activation patterns (Esfahlani et al, 2020) and up-sampling the outcome. While up-sampling does not increase fMRI temporal resolution beyond the acquisition resolution, it permits assessing the pattern of fMRI FC at every 100ms-frame of iEEG without degrading temporal resolution in the latter. This approach permits the EEG connectivity dynamics (and its relationship to fMRI-FC) to be observed over a broad temporal range. To permit sufficient oscillation cycles, oscillation-based connectivity in iEEG was extracted in a window of 4s width anchored at every 100ms, for five canonical frequency bands including: δ (1-4Hz), θ (5-7Hz), α (8-13Hz), β (14-30Hz), and γ (31-60Hz).

Spatial similarity of static connectomes across fMRI and iEEG: We replicated previous reports of spatial association between *static* i.e. time-averaged iEEG-FC and fMRI-FC (Sadaghiani and Wirsich, 2019)(Fig. S2). Consistent with previous work, group-average connectomes in fMRI and source-localized EEG data were significantly correlated across all frequency bands (Fig. S2-A). Similarly in iEEG-fMRI data, the cross-modal association of individual connectomes was significant in group-level statistics. Of note, in line with prior subject-level MEG-to-fMRI comparisons (Hipp and Siegel, 2015), the effect size of this association in individual subjects was small, although statistically significant in most individuals when tested against subject-specific null models (Fig. S2-B). The small albeit significant cross-modal spatial similarity of time-averaged connectomes motivates an important question: to what extent do time-resolved connectome reconfigurations converge/diverge between the two modalities?

Comparison of fMRI and iEEG connectome configurations at synchronous timepoints

To assess the spatiotemporal cross-modal convergence of FC dynamics, we quantified the spatial similarity of FC patterns between fMRI and iEEG-FC_{Amp} at each *synchronous* pairs of frames, i.e. at corresponding

bioRxiv preprint doi: https://doi.org/10.1101/2022.06.17.496647; this version posted June 20, 2022. The copyright holder for this preprint (which was not certified by peer review) is the author/funder, who has granted bioRxiv a license to display the preprint in perpetuity. It is made available under aCC-BY-NC-ND 4.0 International license.

timepoints after compensating for the canonical hemodynamic lag (6s). This *synchronous* frame-wise (every 100ms) spatial correlation (Fig. 2A) yielded a timecourse of cross-modal similarity for each subject and frequency band (see representative subject in Fig. 2B). We tested the significance of the cross-modal correlations at each timepoint against a set of 100 surrogate timeseries generated by spatially phase-permuting the 2D matrix of fMRI-FC at each timepoint (FDR-corrected for all timepoints; $q<0.05$).

Temporally sparse multi-frequency association: The spatial similarity of fMRI and iEEG-FC_{Amp} exceeded chance (comparison to the above-mentioned surrogate data at each timepoint) in a relatively small fraction of frames (from δ to γ, respectively: 5.2±2.0%, 4.4±2.8%, 5.3±3.0%, 4.4±2.2%, 3.8±2.7% of frames). Cumulatively over all electrophysiological frequency bands, a total of 19.2% (±std = 8.1%) of the frames were spatially similar (Fig. 2C). The extracted cross-modal similarity timecourses for the different electrophysiological frequency bands showed low temporal correlation when compared in a pairwise manner; Averaged across subjects, this correlation reached a mean of $r = 0.13 \pm 0.07$ and a maximum of $r = 0.23$ across all pairs of frequency bands (Fig. 2D).

Likelihood of scenarios: The significant spatial similarity of dynamic connectome configurations in fMRI and iEEG speaks against scenario III that posits spatial independence of these configurations. Further, periods of high cross-modal similarity in different electrophysiological frequency bands occurred at largely nonoverlapping times. This observation speaks to a rich multi-frequency association between the FC reconfigurations in the two modalities, rather than presence of a unitary broadband electrophysiological FC process. However, our observations also suggest that the cross-modal spatial similarity occurs sparsely across time even when considering all electrophysiological frequency bands. This sparsity motivates further investigation of the temporal relationship between fMRI-FC and iEEG-FC, to find evidence in support of scenario I or II.

bioRxiv preprint doi: https://doi.org/10.1101/2022.06.17.496647; this version posted June 20, 2022. The copyright holder for this preprint (which was not certified by peer review) is the author/funder, who has granted bioRxiv a license to display the preprint in perpetuity. It is made available under aCC-BY-NC-ND 4.0 International license.

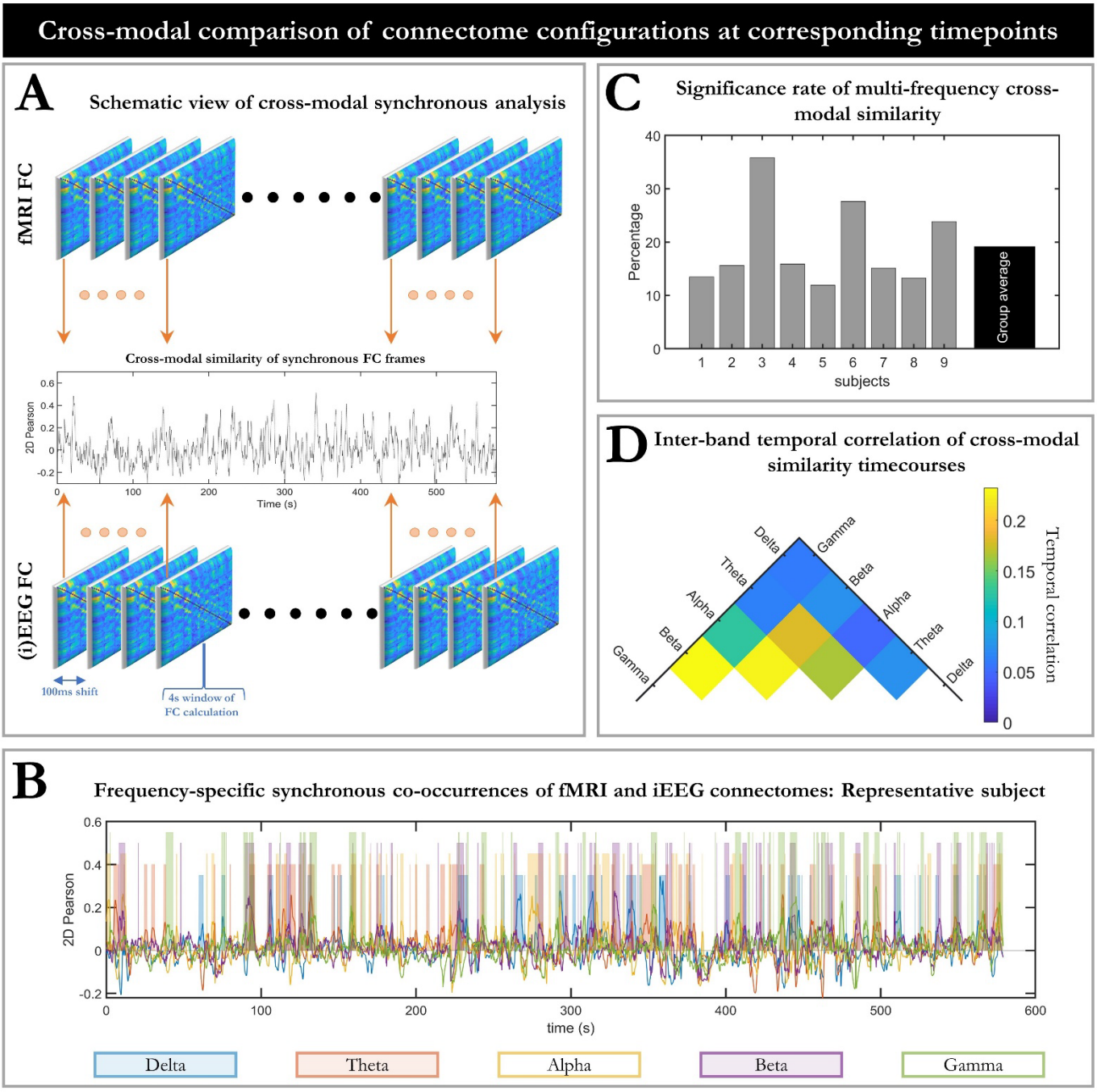

Fig. 2 – ***fMRI and iEEG connectomes spatially converge at intermittent and frequency-specific times.*** *A) A schematic view of the synchronous analysis. For each electrophysiological frequency band and each frame (every 100ms), the spatial similarity was quantified as Pearson correlation across fMRI-FC and iEEG-FC$_{Amp}$ connectome patterns. B) Representative example of the timecourse of similarity between fMRI-FC and iEEG-FC$_{Amp}$ patterns overlaid across all frequency bands (subject #3). For each frequency band, all frames at which correlation values surpass their corresponding chance-level are marked with a transparent bar of the same color (see color coding below the subplot; bars with different heights are used for better visualization). C) For each subject, the percentage of frames that show significant cross-modal similarity in at least one frequency band is depicted. The group average is shown as a blue horizontal line. Spatial convergence was observed in all subjects, speaking against scenario III. However, this convergence occurred during intermittent and relatively sparse epochs. D) Inter-band temporal correlation for the cross-modal spatial similarity timecourses (see subplot B) averaged over the group for the fMRI-FC to iEEG-FC$_{Amp}$ comparison. The small temporal correlation demonstrates a large degree of frequency-specificity of the cross-modal spatial convergence. See Fig. S8 for corresponding results in fMRI-FC and iEEG-FC$_{Phase}$. Taken together, these findings suggest that spatially converging fMRI and iEEG connectome patterns occur at intermittent and frequency-specific times.*

bioRxiv preprint doi: https://doi.org/10.1101/2022.06.17.496647; this version posted June 20, 2022. The copyright holder for this preprint (which was not certified by peer review) is the author/funder, who has granted bioRxiv a license to display the preprint in perpetuity. It is made available under aCC-BY-NC-ND 4.0 International license.

Comparison of fMRI and iEEG connectome configurations at asynchronous timepoints

Likelihood of scenarios: The above-described analyses of fMRI and iEEG at synchronous timepoints suggest the presence of spatially similar connectome patterns, albeit at sparse intervals. This observation makes scenario III (spatial and temporal divergence) unlikely and speaks in favor of scenarios I (spatial and temporal convergence) or II (spatial convergence but temporal divergence). Our observations could align with scenario I if fMRI-derived and iEEG-derived connectome trajectories (sequences of FC patterns) were largely matched but only occasionally reached sufficient proximity (i.e. significant spatial similarity) in our empirical data. Scenario II would provide an alternative explanation for our observations; namely that fMRI and iEEG capture shared FC patterns expressed along temporally independent trajectories. Observing evidence in favor of one versus the other scenario would provide important insights into the neurobiological FC processes captured in the two data modalities; We propose that fMRI- and EEG-derived FC driven by largely shared neurobiological FC processes would be reflected in patterns corresponding to scenario I. Contrarily, observations in line with scenario II would imply the presence of distinct neurobiological FC processes, some captured by fMRI and others by iEEG.

Cross-modal recurrence plot (CRP): To distinguish between scenarios I and II, we investigated the spatial similarity of fMRI and iEEG connectome configurations at all possible pairs of timepoints (i.e. *asynchronous* cross-modal comparison). In other words, we asked whether each fMRI FC frame was spatially similar to each iEEG-FC_{Amp} frame at *any* other timepoint of the recording, and vice versa. This analysis resulted in a 2D matrix of cross-modal spatial correlation values which we call *Cross-modal Recurrence Plot* (CRP; cf. Fig 3A), where matrix entry [*i, j*] corresponds to the spatial correlation of fMRI-FC at time [*i*] to iEEG-FC_{Amp} at time [*j*]. The CRP is similar to previous recurrence plots estimated intra-modally for fMRI (Cabral et al., 2017) but, crucially, investigates *cross-modal* similarity rather than unimodal (self-)similarity over time. For each subject, CRPs were estimated for each electrophysiological frequency band. We then tested the significance of the spatial correlation value at each CRP entry against a set of 100 surrogate correlation values from spatially phase-permuted FC matrices (FDR-corrected). Subsequently, we overlaid significant CRP entries of each electrophysiological frequency band to compare outcomes across frequencies (shown as colored dots for a sample subject in Fig. 3A). We refer to the resulting overlay as multi-frequency CRP. Note that this asynchronous approach overcomes potential imprecision of the 6s hemodynamic lag compensation (see methods).

Off-/on-diagonal ratio of spatially correlated epochs: In the multi-frequency CRP, the on-diagonal entries correspond to synchronous and the off-diagonal entries to asynchronous cross-modal comparisons. To dissociate between scenarios I and II, we focused on the *rate* of spatially convergent epochs in the multi-frequency CRP, where epochs are CRP entries passing significance testing for cross-modal spatial correlation as detailed above. Specifically, we quantified the ratio of off-diagonal to on-diagonal rates (hereinafter "*off-/on-diagonal ratio*") (blue dots in Fig. 3B). In case of scenario I (presence of temporal convergence), given the

bioRxiv preprint doi: https://doi.org/10.1101/2022.06.17.496647; this version posted June 20, 2022. The copyright holder for this preprint (which was not certified by peer review) is the author/funder, who has granted bioRxiv a license to display the preprint in perpetuity. It is made available under aCC-BY-NC-ND 4.0 International license.

expected cross-modal temporal convergence, an off-/on-diagonal ratio considerably smaller than unity would be expected. In case of scenario II however (absence of temporal convergence), given the putative temporal divergence, epochs of spatial similarity between the two modalities could occur equally likely on and off the diagonal. In other words, off-/on-diagonal ratio would not statistically differ from a putative null distribution extracted from randomized multi-frequency CRPs (which is expectedly around 1; see grey dot clouds in Fig. 3B). Thus, to adjudicate the likelihood of scenario I and II, in each subject we compared the off-/on-diagonal ratio to a distribution of null off-/on-diagonal ratios extracted after spatially scrambling the CRP along both temporal axes 100 times (dot clouds in individual columns of Fig. 3B).

Asynchronous cross-modal association: The off-/on-diagonal ratio was close to 1 (mean over subjects ± std = 1.05 ± 0.12). In subject-by-subject non-parametric tests, this ratio was not significantly smaller than the null distribution (Benjamini-Hochberg adjusted *p* values in all subjects >0.98; negative one-tailed test). Although this observation indicates absence of statistical evidence for scenario I (specifically that off-/on-diagonal ratio<1 due to temporal convergence, which we refer to as hypothesis 1 or H1), we applied an additional test to directly assess the probability of H0 (scenario II: off-/on-diagonal ratio≈1 due to temporal divergence) against H1. Specifically, we performed a Bayesian one-tailed group-level paired *t*-test between the real off-/on-diagonal ratios and the subject-specific mean of the null off-/on-diagonal ratios. A BF_{01} (i.e. *Bayes Factor* in favor of H0 over H1) of 5.23 showed that the data are at least five times more likely to occur under H0 than under H1, providing moderate evidence in the direction of H0. Taken together, epochs of cross-modal spatial convergence are equally likely at asynchronous timepoints as they are at synchronous times; corresponding to the lack of an on- vs off-diagonal pattern in the CRP – rather, the dominant pattern consists of horizontal stripes (see below for further discussion). Consequently, epochs of spatial convergence in the asynchronous (CRP) and the synchronous analysis likely arise from *distinct* connectivity processes captured in fMRI and iEEG albeit sharing similar distributed patterns (Scenario II).

Multi-frequency cross-modal association: Overlaying the CRPs of all electrophysiological frequency bands allowed us to study the complimentary nature of the cross-modal relationship in the different bands. The percentage of overlap between frequency-specific significant CRP epochs (Jaccard index) is visualized for all pairs of frequencies in Fig. 3C. Across all pairs of frequency bands, there was only small overlap between the single-frequency CRPs (Jaccard index reaching at most 0.09±0.04 for α- vs. β-band CRPs). In line with observations from the synchronous analysis, this result demonstrates that the spatial similarity of fMRI-FC to the different electrophysiological bands occurs at largely different (pairs of) timepoints. In other words, band-specific iEEG connectome patterns are associated with fMRI-FC configurations in a complimentary manner, corresponding to a refined scenario II of Fig. 1 with multiple distinct state trajectories for the different iEEG bands.

bioRxiv preprint doi: https://doi.org/10.1101/2022.06.17.496647; this version posted June 20, 2022. The copyright holder for this preprint (which was not certified by peer review) is the author/funder, who has granted bioRxiv a license to display the preprint in perpetuity. It is made available under aCC-BY-NC-ND 4.0 International license.

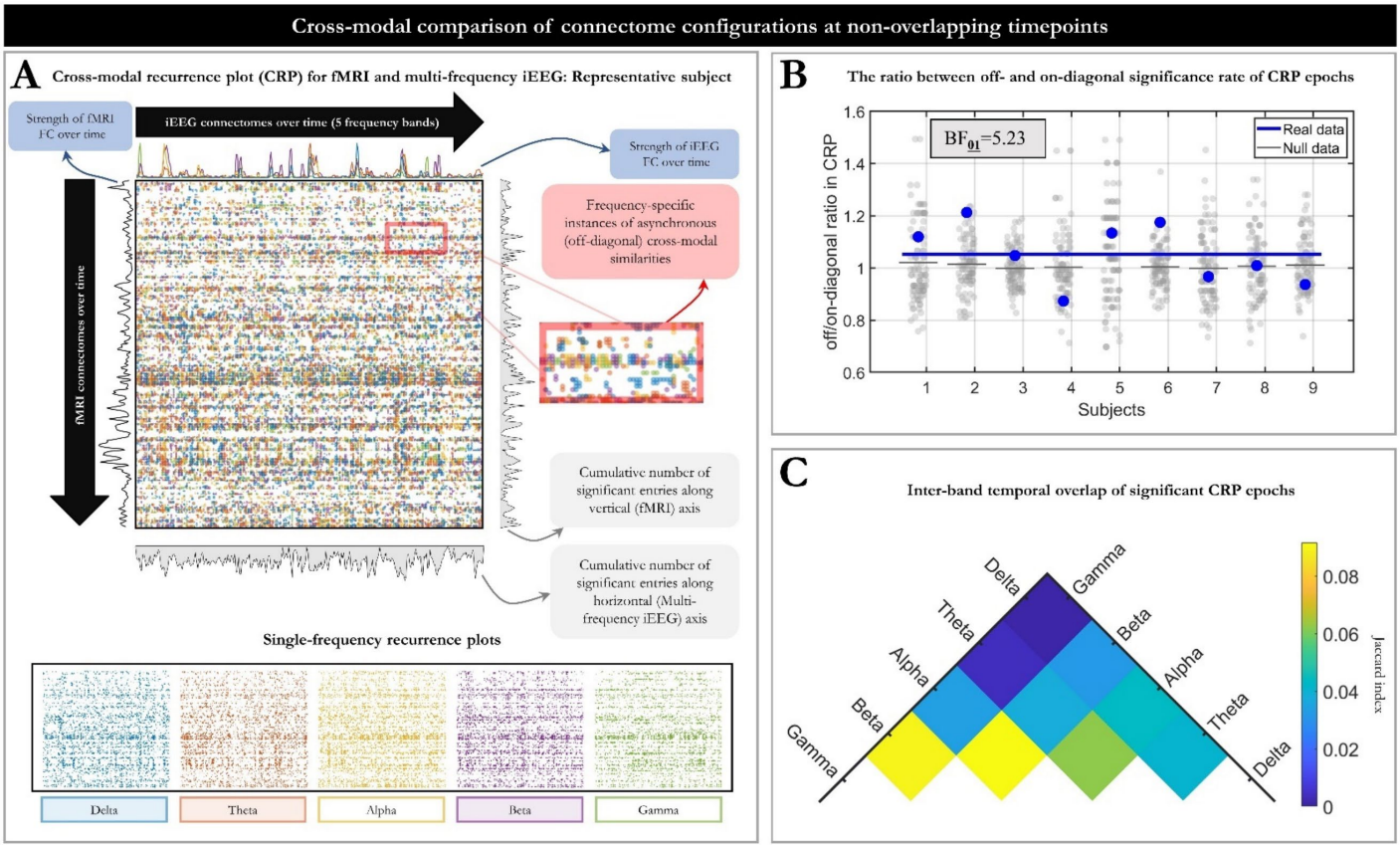

Fig. 3 – ***The spatial convergence across fMRI and frequency-specific iEEG connectomes occurs asynchronously.*** *A) Cross-modal recurrence plot (CRP) between fMRI-FC (time running along y axis from top to bottom) and iEEG-FC$_{Amp}$ (time running along the x axis from left to right) overlaid for the different electrophysiological bands for subject #3. Note that synchronous observations fall on the diagonal of the CRP and correspond directly to the data shown in Fig. 2B. In addition to the overlay, the CRPs of the individual frequency bands (color-coded) are provided separately at the bottom of the panel. Each CRP is thresholded (binarized) in comparison to the corresponding frequency-specific null model generated from spatially phase-permuted FC matrices, Benjamini-Hochberg FDR-corrected for the number of all pairs of timepoints. Specifically, pairs of timepoints with significant spatial correlation across fMRI and iEEG FC are indicated with color-coded dots for each frequency band (See red box for a magnified section). The cumulative number of significant epochs along rows and columns of the CRP are shown in the bottom and right side of the CRP, respectively. The strength of fMRI-FC and iEEG FC (measured as Root Sum Square) are shown on the left side and top of the CRP, respectively, and were not associated with cross-modal similarity (see section addressing alternative sources of contribution). B) We focus on the rate of epochs with significant spatial correlation in the multi-frequency CRP. The off- over on-diagonal ratio of this rate is shown for all nine subjects (blue circles). The blue line represents the group-level average. Gray dot clouds show null distributions of off-/on-diagonal ratios extracted from spatially-randomized CRPs, while black lines show the subject-specific mean of the null ratios. The off-/on-diagonal ratio in each individual subject was statistically indistinguishable from the corresponding null distribution. Bayesian group-level statistics showed >five times higher likelihood for the absence of difference in the rate of spatially correlated epochs off-diagonal and on-diagonal (BF$_{01}$=5.23). This observation demonstrates that significant spatial correlation across iEEG and fMRI FC occurred equally likely at asynchronous (off-diagonal) and synchronous (on-diagonal) timepoints. C) Degree of overlap between pairs of frequency-specific thresholded CRPs (as shown at the bottom of A), expressed as group-average of the Jaccard index. The low values (cf. possible index range of 0-1) demonstrate that timepoint pairs of high cross-modal spatial correlation are largely distinct across different electrophysiological frequency bands. In summary, the observed cross-modal spatial convergence at frequency-specific and asynchronous epochs suggests that connectome dynamics across different FC timescales traverse spatially similar patterns asynchronously (Scenario II).*

Attractors for the cross-modal association: Another prominent characteristic of the multi-frequency CRPs is the emergence of prominent horizontal stripes when significant CRP epochs are aggregated across all frequency bands (illustrative case shown in Fig. 3A). While there is also a degree of vertical stripiness in some CRPs, we quantitatively established the prominence of horizontal CRP stripes in 7/9 iEEG-fMRI and 25/26 source-

bioRxiv preprint doi: https://doi.org/10.1101/2022.06.17.496647; this version posted June 20, 2022. The copyright holder for this preprint (which was not certified by peer review) is the author/funder, who has granted bioRxiv a license to display the preprint in perpetuity. It is made available under aCC-BY-NC-ND 4.0 International license.

localized EEG-fMRI datasets (Fig. S3A). Each stripe corresponds to a brief period, during which the fMRI-derived connectome configuration contains a connectivity pattern that is stably present (over time) in the iEEG connectome in one or more of the frequency bands. We quantitatively confirmed that the stripes largely correspond to the stable, i.e. static, component of EEG FC organization (Fig. S3B-C). Specifically, we demonstrated the emergence of equivalent stripes in multi-frequency "pseudo-CRPs" derived from the original fMRI-FC timeseries and a *constant* timeseries of the time-averaged (static) EEG connectome. These observations imply that the intrinsic FC component of EEG serves as an attractor for the cross-modal spatiotemporal convergence. The considerable number of significant CRP epochs outside the stripes, however, raises the question of whether fMRI and iEEG share spatial patterns distinct from the static connectome attractor, possibly in the form of dissociable recurrent states. To identify such putative connectome states at the group level, we leveraged the whole-brain coverage of the source-localized EEG-fMRI dataset using clustering (see section "Cross-modally converging connectome states" below). To this end however, we first demonstrate that our major findings extend to the source-localized EEG-fMRI dataset in the next section.

Generalization to source-localized EEG-fMRI: whole-brain connectomes in healthy subjects

To validate our results in the whole-brain connectome and in subjects without neurological disorders, we sought to extend our findings to a resting state concurrent source-localized EEG-fMRI dataset composed of 26 healthy subjects (Fig. 4). EEG connectomes were derived from data source-localized to the Desikan-Killiany atlas (Desikan et al., 2006), uncorrected for leakage and replicated in (leakage corrected) source-orthogonalized data (Fig. S5).

Synchronous analyses: In line with the iEEG-fMRI findings, a relatively small proportion of synchronous connectome frames showed significant correlations between fMRI-FC and EEG-FC_{Amp} in each frequency band, reaching 30.6 ± 7.8% when pooled across all bands (Fig. 4A). Note that this proportion was higher than in the intracranial data possibly due to a more complete coverage of the connectome. Similar to the intracranial data, the frequency-specific cross-modal similarity timecourses showed only small temporal dependence across pairs of frequency bands, emphasizing the multi-frequency nature of the cross-modal link ($r = 0.19 \pm 0.07$; Fig. 4B).

Asynchronous analyses: Similarly, the asynchronous analysis and ensuing CRPs confirmed observations of the intracranial dataset (a sample subject is shown in Fig. 4C). The group-average off-/on-diagonal ratio was 1.01 ± 0.10 (Fig. 4D). In 25 of 26 individuals, the off-/on-diagonal ratio was not significantly smaller than chance level when compared to 100 subject-specific spatially phase-randomized CRPs (Benjamini-Hochberg adjusted p values across subjects >0.26; shown in individual columns in Fig. 4D). An additional Bayesian negative one-tailed paired t-test with a BF_{01} of 6.54 directly provided evidence that scenario II (H0) is six times more likely than scenario I (H1) given the data. This observation emphasizes the distinctness of the FC processes captured by the two modalities. The value of the Jaccard index for the overlap of significant epochs across frequency-

bioRxiv preprint doi: https://doi.org/10.1101/2022.06.17.496647; this version posted June 20, 2022. The copyright holder for this preprint (which was not certified by peer review) is the author/funder, who has granted bioRxiv a license to display the preprint in perpetuity. It is made available under aCC-BY-NC-ND 4.0 International license.

specific CRPs was low (maximum value: 0.14±0.05 for β- vs. γ-band CRPs; Fig. 4E), speaking to the multi-frequency nature of the association between fMRI and EEG connectome dynamics. In summary, these findings are in line with our invasive observations in patients with epilepsy.

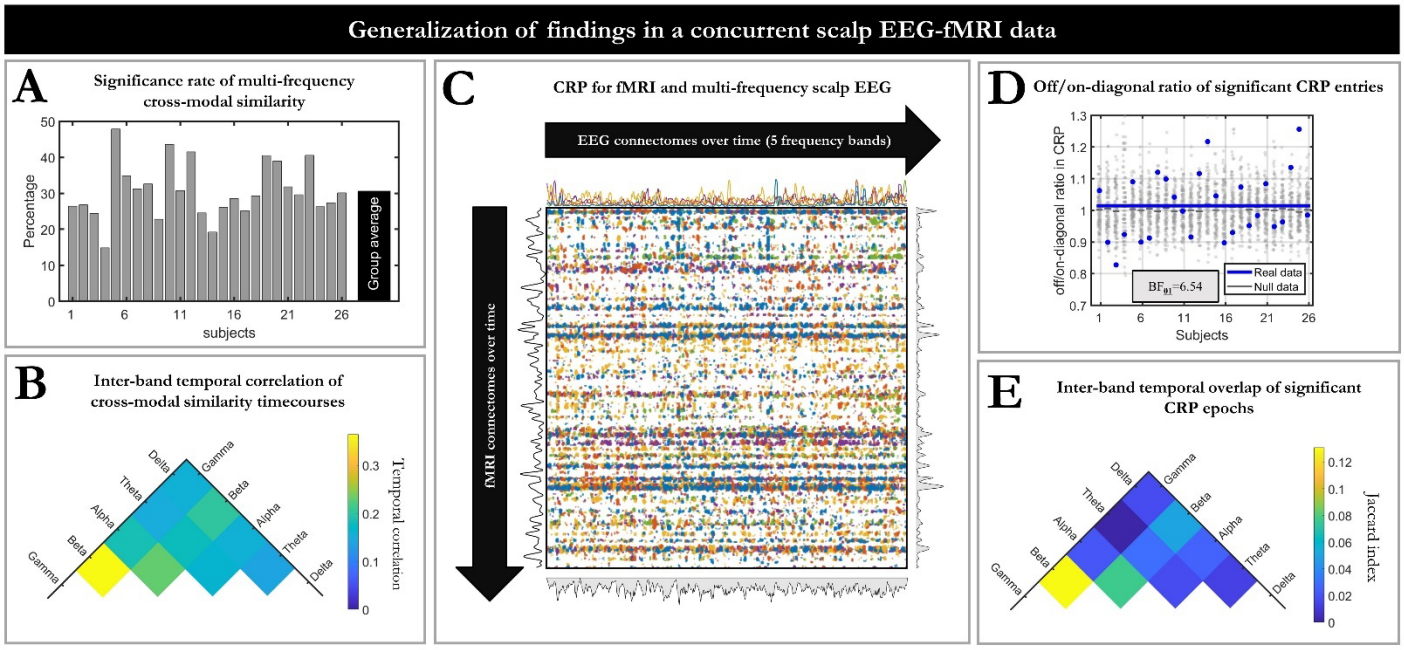

Fig. 4 – ***Findings generalize to the whole-brain connectome of healthy subjects based on concurrent source-localized EEG-fMRI.*** *A) Total significance rate of the cross-modal similarity timecourse when aggregated across all frequency bands, shown across all subjects (**N = 26;** analogous to Fig. 2C). B) Temporal overlap of frequency-specific cross-modal similarity timecourses in a pairwise manner (analogous to Fig. 2D). C) An example of multi-frequency CRP shown for one subject (analogous to Fig. 3A). D) The off-/on-diagonal ratio of the rate of spatially correlated epochs in the multi-frequency CRP for all individual subjects (analogous to Fig. 3B). E) Overlap of spatially correlated epochs across pairs of electrophysiological frequencies in the multi-frequency CRP (averaged over subjects; analogous to Fig. 3C). Equivalent findings are presented for EEG phase coupling connectomes as a supplemental analysis.*

Cross-modally converging connectome states

In this section we investigate the spatial characteristics of the cross-modally shared spatial patterns alluded to in the CRP analysis. In particular, we ask whether the shared connectome space in scenario II primarily reflects random (i.e. nonrecurrent and cross-modally unrelated) variations around the cross-modally shared spatial pattern of the static connectome attractor (see characterization of CRP stripes above), or additionally contains a shared set of distinct connectome states. To address this question, we aimed to show that I) the significant CRP entries can be categorized into dissociable sets of recurrent connectome states in each modality, and II) that these connectome states compose distinct pairs of states across EEG and fMRI. Note that here we exclusively focus on the source-localized EEG-fMRI dataset since its coverage permits observation of whole-brain connectome states and the embedded canonical intrinsic connectivity networks that are shared across subjects, whereas the partial intracranial EEG electrode coverage differs between subjects.

bioRxiv preprint doi: https://doi.org/10.1101/2022.06.17.496647; this version posted June 20, 2022. The copyright holder for this preprint (which was not certified by peer review) is the author/funder, who has granted bioRxiv a license to display the preprint in perpetuity. It is made available under aCC-BY-NC-ND 4.0 International license.

I. Dissociable connectome states in each modality

In each frequency-specific CRP, we pooled the connectivity matrices at all significant epochs across individuals. Then, separately in each data modality, we grouped the connectivity matrices into clusters using K-means clustering for k=4 to 10 clusters. The optimal number of clusters determined by the Calinski Harabasz index, k^*, was found to be 4 for fMRI in all frequency-specific CRPs, k^*=4 for the δ-, α- and γ-band CRPs, k^*=5 in the θ-band CRP, and k^*=7 in β-band CRP. Group-level whole-brain connectome states (cluster centroids) of fMRI and θ-band EEG (i.e. from the θ-band CRP) are visualized in Fig. 5A as an example (See Fig. S6 for other frequency bands).

Within each modality, we statistically assessed distinctness of connectome states by showing that their state centroids are more dissimilar than randomly assigned state centroids. Specifically, we tested the spatial correlation across every pair of state centroids of each modality (from a given frequency-specific CRP) against a null distribution of correlations generated from 100 pseudo-state centroid correlations ($q < 0.05$ FDR-corrected for the number of state pairs). Pseudo-states were generated from Monte-Carlo permutations of state labels (of the connectome frames from the original state pair).

Dissociable states within fMRI data: The average spatial correlation across all pairs of state centroids in fMRI was equal to 0.39±0.10, 0.40±0.07, 0.40±0.11, 0.35±0.09, and 0.36±0.09 (from δ-band CRP to γ-band CRP). In contrast, corresponding null values were equal to 1.00±0.00 for all frequency-specific CRPs, because random clustering of connectome configurations extracts what is common across all epochs, i.e. the static FC organization (thus generating cluster centroids that are indistinguishable from the static connectome and from each other).

Dissociable states within EEG data: Similar results were observed for EEG connectome states across all frequency-specific CRPs (correlation across real cluster centroids: 0.49±0.15, 0.47±0.11, 0.57±0.11, 0.34±0.19, and 0.36±0.13; correlation of pseudo-state centroids: 1.00±0.00, for all frequency-specific CRPs).

These observations speak to the presence of dissociable connectome configurations in both modalities, each providing a basis for cross-modal spatial convergence beyond the shared static FC organization.

II. Distinct connectome state matches across modalities

Although the connectome states in each modality are statistically dissociable, they are spatially moderately correlated to one another since they all reflect features of the static FC organization to some degree. Thus, we asked whether the cross-modal spatial convergence corresponds to *crossmodally-matched* states of EEG and fMRI. If so, such cross-modal matches should make up a large proportion of the spatially correlated epochs. Alternatively, in the absence of unique cross-modal state matches, the observed connectome states would randomly pair with one another (i.e. with uniform frequency).

Distinct crossmodally-matched connectome states: To discriminate between these two possibilities, we counted how often each fMRI state paired up with each EEG state among all spatially correlated epochs (for each

bioRxiv preprint doi: https://doi.org/10.1101/2022.06.17.496647; this version posted June 20, 2022. The copyright holder for this preprint (which was not certified by peer review) is the author/funder, who has granted bioRxiv a license to display the preprint in perpetuity. It is made available under aCC-BY-NC-ND 4.0 International license.

frequency-specific CRP). For all pairs of fMRI and EEG states, we compared this count to a null model generated from randomly permuted EEG cluster labels (5000 repetitions; corrected for all possible state pairs). In each frequency-specific CRP, we indeed observed cross-modal connectome state matches that occurred considerably more often than chance, as expressed in the high z-scores in Fig. 5B. For each of the four fMRI states (separately in each frequency-specific CRP), we identified the strongest EEG state match, highlighted as the largest disk at each row of the lattices in Fig. 5B. The state centroids of the matches are exemplified for the θ-band CRP in Fig. 5A. Remarkably, this procedure resulted in a largely exclusive EEG state match for each fMRI state, with the only exceptions being a double match in α and γ bands. The significant prevalence and exclusive nature of cross-modal state matches imply that the observed asynchronous spatial convergence is not merely due to the shared static FC organization, but rather comprises cross-modally shared, distinct and recurrent connectome states.

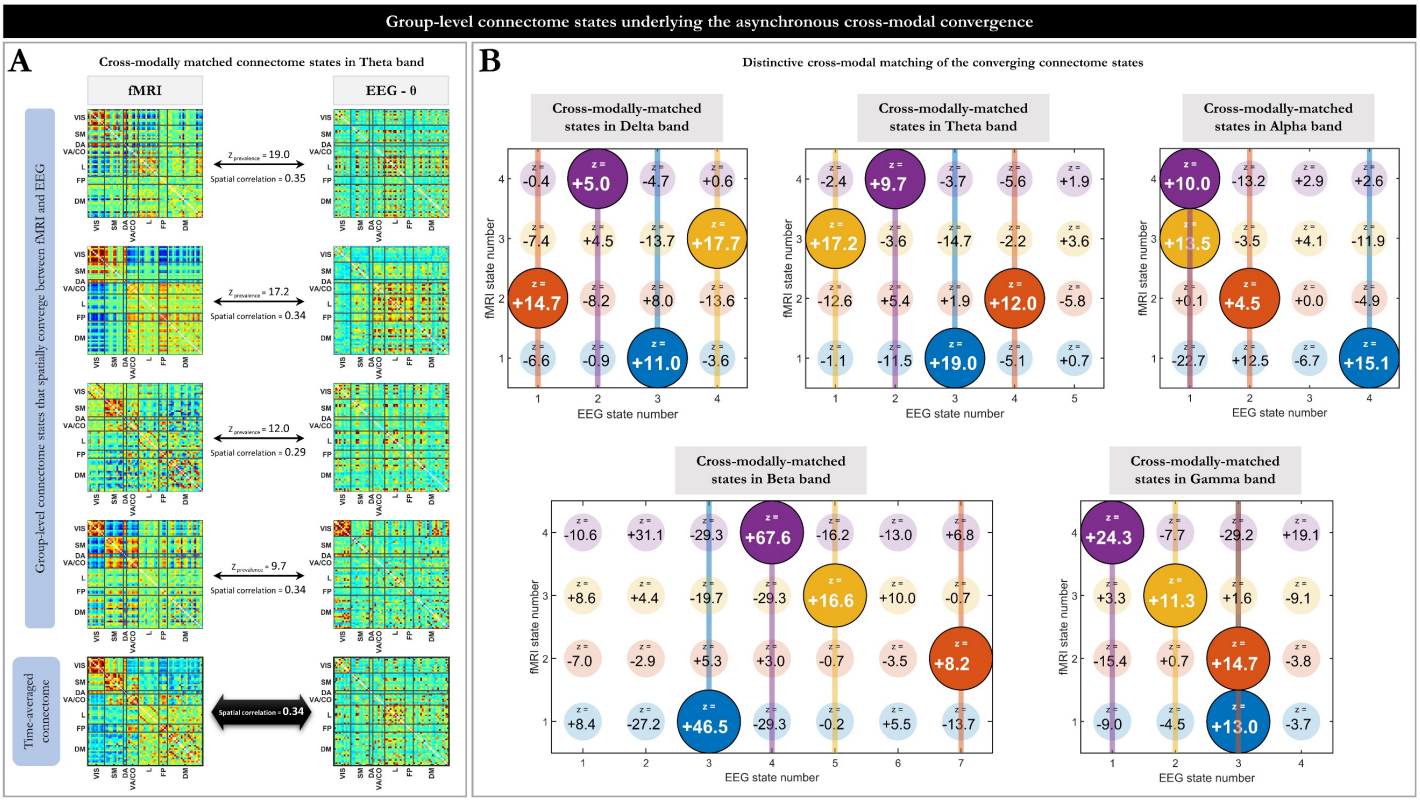

*Fig. 5 – **The asynchronous spatial correlation between fMRI and EEG connectome patterns arises from distinct pairs of connectome states**. A) Illustration of four distinct pairs of fMRI (left) and θ band EEG (right) group-level connectome states, derived from the θ-band CRP epochs with significant cross-modal spatial correlation (cf. Fig. 3A). For comparison, we also provide the time-averaged fMRI and θ-band EEG connectomes at the bottom. Connectomes are organized into the following seven canonical intrinsic connectivity networks (ICNs): VIS (Visual), SM (Somatomotor), DA (Dorsal Attention), VA/CO (Ventral Attention or Cingulo-opercular), L (Limbic), FP (Fronto-Parietal), and DM (Default Mode) networks (Yeo et al., 2011). The side-by-side fMRI and EEG state pair in each row demonstrates particularly high prevalence of pairing in the CRP. This prevalence is quantified on the arrows as Z-scores (in comparison to a null distribution) and sorted from top to bottom for the most to least strong pairing. Spatial correlation for each state pair is depicted under the corresponding arrows. Note that state pairs show sets of ICNs in/across which FC is relatively over-represented in both data modalities compared to the static FC organization (e.g. state pair one: L; state pair four: VIS & DA). B) Z-score values of state matching depicted for all possible state pairs across all frequency bands (the four larger disks in θ band correspond to the four state matches depicted in A). Large disks at every row indicate the strongest EEG state match (Z-score in comparison to the null distribution) for the corresponding fMRI state. Remarkably, the EEG state matches of each fMRI state are largely exclusive, with the exception of a double match in α- and γ-band CRPs. The significant prevalence and largely exclusive*

bioRxiv preprint doi: https://doi.org/10.1101/2022.06.17.496647; this version posted June 20, 2022. The copyright holder for this preprint (which was not certified by peer review) is the author/funder, who has granted bioRxiv a license to display the preprint in perpetuity. It is made available under aCC-BY-NC-ND 4.0 International license.

Addressing alternative sources of contribution

We observed a sparse asynchronous association between fMRI and iEEG/EEG connectome states across all timescales. Such sparse cross-modal convergence could in principle arise from various factors, other than genuine divergence of connectome reconfigurations due to distinctness of neural processes across timescales. Given that the *static* (time-averaged) connectome organization of fMRI and iEEG/EEG are correlated (Wirsich et al., 2021), such sparse cross-modal convergence could simply reflect the degree to which the cross-modally shared static connectome organization is expressed in one or the other modality. Contrarily, a supplemental analysis demonstrated that the degree to which fMRI or EEG frame-by-frame connectome configurations correlate with the static connectome of the respective modality is not associated with cross-modal similarity of the configurations (section II of supplementary materials). Further, one could argue that signal-to-noise ratio (SNR) in estimation of FC or other common artifacts such as head motion, epileptiform activity (for intracranial data), and volume conduction (for scalp data) may drive the observed sparse association between the two modalities. We tested the effects of each of these factors on our findings and found no significant effect in either of the datasets (section II of supplementary materials). The independence of our findings from such artifacts speaks to genuine temporal divergence of (spatially shared) connectome reconfigurations across timescales.

Connectome-level vs. connection-level convergence

Prior literature supports the existence of an electrophysiological basis for fMRI FC dynamics (Wirsich et al., 2020b; Zhang et al., 2020). Therefore, our findings of temporally divergent fMRI and EEG connectome trajectories may appear to contradict this prior work. Importantly however, this prior literature assessed the temporal relationship of FC across fMRI and EEG in a connection-wise manner (i.e. at the level of individual connections) rather than the largescale spatial pattern of connectivity, which is a novel contribution of the current work. To confirm the existence of such connection-level electrophysiological basis for fMRI FC fluctuations, we replicated the known connection-level temporal convergence in our intracranial EEG-fMRI data. We found significant cross-modal temporal association in a substantial proportion (albeit not all) of individual connections over all frequency bands (Fig. S4). Our findings confirm the existence of electrophysiological correlates of fMRI FC dynamics at the level of individual connections, while suggesting presence of independent connectome trajectories across the two modalities.

bioRxiv preprint doi: https://doi.org/10.1101/2022.06.17.496647; this version posted June 20, 2022. The copyright holder for this preprint (which was not certified by peer review) is the author/funder, who has granted bioRxiv a license to display the preprint in perpetuity. It is made available under aCC-BY-NC-ND 4.0 International license.

Discussion

We set out to quantify the degree of association/dissociation between the functional connectomes derived from electrophysiological recordings and fMRI in humans using a spatiotemporal dynamic analysis framework. We showed that hemodynamics- and electrophysiology-derived connectivity express spatially shared but temporally asynchronous connectome patterns consistent with scenario II, one of the three proposed possible scenarios (Fig. 1). This was observed in two independent, multimodal datasets: concurrent fMRI with EEG recorded intracranially, and with EEG recorded on the scalp. Furthermore, through clustering we identified that the spatial convergence constitutes crossmodally-matched *recurrent* connectome states. Additionally, our findings suggest that the cross-modal association is frequency-dependent: fMRI-connectome patterns spatially converge with EEG patterns of different electrophysiological frequencies at largely non-overlapping timepoints.

We may deduce from the above conclusions (i.e. scenario II) that it seems unlikely that hemodynamics- and frequency-specific electrophysiology-derived connectivity reconfigurations reflect a single underlying process. In particular, if fMRI and EEG merely provided two different but complementary windows onto the same underlying neurophysiological connectivity processes, one would expect these processes to appear in the two data modalities around the same time. The alternative view, based on our preceding observations of *asynchronous* spatially overlapping connectome patterns is in line with the viewpoint that each modality is more sensitive to different aspects of neural processing. More specifically, Hari and Parkkonen (2015) argue that although electrophysiological data better capture neural activity involving fast-conducting (thick, myelinated) fibers, fMRI data prominently reflects neural ensembles connected via slow (thin, unmyelinated) fibers. According to this viewpoint, each type of neural activity, slow and fast, subserves cognitive processes at different speeds suggesting that each modality better captures particular aspects of behavioral neural correlates (Hari and Parkkonen, 2015). We have recently suggested that the functional connectome may comprise distinct spatial patterns of connectivity that unfold at different timescales (Wirsich et al., 2020a; Sadaghiani et al., 2022). These connectome patterns could dominate the signals in hemodynamic and electrophysiological acquisition methods, respectively. This perspective could also explain why hemodynamics- and oscillation-based connectomes, in time-averaged or short window investigations, are limited in their spatial similarity which rarely surpasses a small to moderate effect size (Betzel et al., 2019; Wirsich et al., 2021), (Fig. S2).

Multi-modal studies have predominantly aimed at cross-validating intrinsic processes in hemodynamic and electrophysiological data by comparing their strength or temporal evolution, often at the level of regional activation (Mukamel et al., 2005; Nir et al., 2007) or connection-wise FC (Kucyi et al., 2018; Zhang et al., 2020), the latter including studies of the iEEG-fMRI and scalp EEG-fMRI data used in the current study (Ridley et al., 2017; and Wirsich et al., 2020b, respectively). In contrast to this prior work, the current study investigated the cross-modal temporal relationship at the level of connectome patterns distributed over *all* available

bioRxiv preprint doi: https://doi.org/10.1101/2022.06.17.496647; this version posted June 20, 2022. The copyright holder for this preprint (which was not certified by peer review) is the author/funder, who has granted bioRxiv a license to display the preprint in perpetuity. It is made available under aCC-BY-NC-ND 4.0 International license.

connections. We observed a *connectome-level* temporal divergence in this study which may contrast the *connection-level* temporal convergence of FC reported in the above-described studies. The apparent discrepancy may be explained by the presence of distinct neural processes driving the connection-wise and connectome-wise FC changes in the two modalities. Indeed, we confirmed existence of infraslow electrophysiological FC fluctuations driving cross-modal temporal associations at the level of individual connections (Fig. S4), which likely differ from the FC processes underlying rapidly emerging and dissolving distributed spatial patterns in each modality at the connectome level. Of note, we found significant temporal associations across many but not all connections (cf. Fig. S4), leaving room for dissociation at the level of large-scale FC patterns. Generative models may shed light on the factors underlying the dissociation of connectivity processes at the level of connectome patterns versus individual connections (Deco et al., 2009; Cabral et al., 2014; Rabuffo et al., 2021).

Another core conclusion pertains to the rich multi-frequency signature of the cross-modal relationship. Specifically, in both synchronous and asynchronous approaches, hemodynamic FC configurations spatially converged with electrophysiological FC patterns in all canonical frequency bands and did so at largely non-overlapping timepoints across bands. Similarly, in our clustering approach, all four fMRI connectome states matched with specific EEG connectome states in each frequency band, rather than individual fMRI states being tied to specific EEG frequency bands. These observations suggest that electrophysiological connectome dynamics do not constitute a unitary, broad-band FC process, but rather a set of frequency-specific FC processes unfolding in a dissociable and complimentary manner. This interpretation is further supported by our independent, unimodal (iEEG) study, showing that the connection-wise temporal dynamics of oscillation-based FC are independent across frequency bands (Mostame and Sadaghiani, 2020a). From a functional perspective, temporally dissociable connectome reconfigurations in different frequency bands could constitute parallel "communication channels" across which brain regions interact with multiple sets of other brain regions via oscillations at different frequencies.

Viewing canonical frequencies from a complimentary perspective reveals another prominent feature of the cross-modal relationship. Specifically, in the multifrequency CRP we observed horizontal stripes constructed from non-overlapping frequency-specific epochs of cross-modal spatial convergence. This finding implies that at particular timepoints, the fMRI-derived connectome configuration spatially converges with a component in EEG connectomes that is shared across frequency bands over a large proportion of timepoints. Such findings from the dynamic domain provides insight into the static domain (Tewarie et al., 2016). Tewarie demonstrated that considering FC matrices of all canonical frequency bands collectively, as opposed to individually, improved prediction of the (group-average) fMRI-derived static connectome. This dovetails with our findings, which suggests that moment-to-moment connectome configurations in individual frequencies each contribute to the static fMRI-derived connectome organization at independent timepoints. In other words, the static fMRI-

bioRxiv preprint doi: https://doi.org/10.1101/2022.06.17.496647; this version posted June 20, 2022. The copyright holder for this preprint (which was not certified by peer review) is the author/funder, who has granted bioRxiv a license to display the preprint in perpetuity. It is made available under aCC-BY-NC-ND 4.0 International license.

derived connectome organization comprises the cumulative pattern of all temporally dissociated frequency-specific electrophysiological FC states "compressed" into a time-averaged architecture.

A common basis for the cross-modal spatial convergence is likely the structural connectome. Several studies have shown that the core, time-averaged architecture of oscillation-based FC is correlated with the structural connectivity scaffold in both empirical data (Deligianni et al., 2016; Wirsich et al., 2017; Betzel et al., 2019) and dynamic whole-brain generative models based on diffusion MRI connectivity (Cabral et al., 2017). Therefore, the shared structural connectivity likely drives spatial similarity of connectome states across fMRI and EEG particularly at timepoints where the fMRI configuration results in CRP stripes. Critically however, there exist many asynchronous epochs of spatially similar fMRI and EEG connectome configurations outside of the CRP stripes when the dynamics stray from the static structural foundation. In particular, we identified exclusive cross-modal pairs of recurrent connectome states that spatially differed from the static scaffold. This observation suggests that cross-modal association is not limited to the static FC pattern of a functional modality or the underlying structural organization.

Our findings are in line with scenario II described in Fig. 1, but with the refined view that state trajectories are largely temporally independent not only across data modalities (hemodynamic vs. electrophysiology) but also across band-specific oscillations. Taken together, these findings suggest that fMRI and EEG connectomes provide complimentary information about dynamics of large-scale neural communication that is likely rooted in a shared foundation of static functional connectivity.

Limitations

The hemodynamic response of the brain bounded the temporal resolution of the results. However, this methodological limitation of fMRI may produce high sensitivity to particularly slow brain processes (Hari and Parkkonen, 2015). Similarly, while the temporal resolution of iEEG connectivity was high, it was subject to the temporal smoothing effect of the estimation window. Oscillation-based connectivity requires several oscillation cycles to yield a reliable connectivity estimate thus necessitating an estimation window of several seconds in continuous recordings. While the EEG estimation window may be considered a methodological limitation, it aligns with the neurobiological viewpoint that several oscillation cycles are needed for cross-region synchronization to be functionally effective.

Another consideration is that we could not reliably investigate high-frequency broadband ("high-γ" band; >60 Hz) range, because concurrently recorded iEEG is disproportionately affected by MR-related artifacts in higher frequencies (Mullinger and Bowtell, 2011; Mele et al., 2019). The limited spatial sampling (coverage) of iEEG electrodes in epileptic patients -dictated by clinical considerations- is another important limitation. Nonetheless, we were able to replicate our findings in the absence of such limited spatial sampling by leveraging whole-brain source-localized EEG-fMRI recordings. In iEEG data, volume conduction effects are minimal (Rouse et al., 2016; Dubey and Ray, 2019) and in the source-localized EEG recordings source leakage correction was

bioRxiv preprint doi: https://doi.org/10.1101/2022.06.17.496647; this version posted June 20, 2022. The copyright holder for this preprint (which was not certified by peer review) is the author/funder, who has granted bioRxiv a license to display the preprint in perpetuity. It is made available under aCC-BY-NC-ND 4.0 International license.

performed (Colclough et al., 2015). It should be noted however that even state-of-the-art volume conduction mitigation strategies cannot distinguish artefactual zero-phase lag from genuine zero-phase lag neural activity. To mitigate this issue, we provide results from source-localized data both with and without leakage correction (supplementary and main text, respectively).

Conclusions

Capitalizing on resting-state concurrent intracranial EEG and fMRI data in humans, we have shown that fMRI and iEEG connectomes exhibit spatially similar patterns of connectivity, at different times, potentially driven by distinct neurobiological connectivity processes. This pattern was also observed in concurrent source-localized EEG and fMRI data in healthy subjects. Our observations —that reconfigurations of FC at the different timescales of fMRI and iEEG are mostly independent— is consistent with the viewpoint that BOLD and electrophysiological signals may preferentially capture different neural populations composed of distinct axonal diameters, myelination, and neurotransmitters (Hari and Parkkonen, 2015). Accordingly, fMRI- and electrophysiology-derived connectivity may be envisaged as distinct aspects of brain function rather than as exclusively intermodal measurements of the same phenomenon. From this perspective, the functional connectome is reconceptualized as a composite process that engages recurrent configurations across a maximally broad range of timescales across a shared spatial organization. This conclusion further motivates interrogating connectome dynamics across a range of temporal scales.

Methods

This study utilized two independent datasets: 1) concurrent fMRI and intracranial EEG resting state recordings of 9 subjects with drug-resistant epilepsy, and 2) concurrent fMRI and source-localized EEG resting state recordings of 26 healthy subjects. Findings established in the first dataset under conditions of minimal volume conduction were subsequently generalized to whole-brain connectomes. Note these datasets comprise different (clinical and non-clinical) populations and were acquired with different hardware and imaging sequences.

Data and subjects

Intracranial EEG-fMRI dataset: The data has been originally introduced elsewhere (Ridley et al., 2017). Briefly, nine patients (average 30.4 ± 4.5 years; range 24–38; three females) undergoing presurgical monitoring for treatment of intractable epilepsy gave informed consent according to procedures approved by the Joint Research Ethics Committee of the National Hospital for Neurology and Neurosurgery (NHNN, UCLH NHS Foundation Trust) and UCL Institute of Neurology, London, UK.

Data acquisition is detailed in (Ridley et al., 2017). Briefly, fMRI data was acquired using a 1.5T Siemens Avanto scanner with a GE-EPI pulse sequence (TR = 3 s; TE = 78 ms; 38 slices; 200 volumes; field of view: 192×192; voxel size: 3×3×3 mm^3). Structural T1-weighted scan were acquired using a FLASH pulse sequence

bioRxiv preprint doi: https://doi.org/10.1101/2022.06.17.496647; this version posted June 20, 2022. The copyright holder for this preprint (which was not certified by peer review) is the author/funder, who has granted bioRxiv a license to display the preprint in perpetuity. It is made available under aCC-BY-NC-ND 4.0 International license.

(TR = 3 s; TE = 40 ms; 176 slices; field of view: 208×256; voxel size: 1×1×1.2 mm^3). Intracranial EEG was recorded using an MR-compatible amplifier (BrainAmp MR, Brain Products, Munich, Germany) at 5kHz sampling rate. Number of electrodes (ECoG (grid/strip) and depth electrodes) and the associated fMRI regions of interest (ROIs) that were included in our analysis was on average ~37 (Min = 11; Max = 77; Median = 36). Fig. 1 shows the location of the implanted depth and ECoG electrodes for each subject. The data was acquired during a 10-minutes resting state scan (except for subject P05: ~5 minutes). Subjects were instructed to keep their eyes open.

Source-localized EEG-fMRI dataset: The data has been originally introduced elsewhere (Sadaghiani et al., 2010). Briefly, 10 minutes of eyes-closed resting state were recorded in 26 healthy subjects (average age = 24.39 years; range: 18-31 years; 8 females) with no history of psychiatric or neurological disorders. Informed consent was given by each participant and the study was approved by the local Research Ethics Committee (CPP Ile de France III). FMRI was acquired using a 3T Siemens Tim Trio scanner with a GE-EPI pulse sequence (TR = 2 s; TE = 50 ms; 40 slices; 300 volumes; field of view: 192×192; voxel size: 3×3×3 mm^3). Structural T1-weighted scan were acquired using the MPRAGE pulse sequence (176 slices; field of view: 256×256; voxel size: 1×1×1 mm^3). 62-channel scalp EEG (Easycap, with an additional EOG and an ECG channel) was recorded using an MR-compatible amplifier (BrainAmp MR, Brain Products) at 5Hz sampling rate.

Data preprocessing

Intracranial EEG-fMRI dataset: The fMRI data was preprocessed as explained in (Ridley et al., 2017). Briefly, for each subject, common fMRI preprocessing steps were performed in SPM8 (https://www.fil.ion.ucl.ac.uk/spm/software/spm8/) (Respectively: slice time correction, realignment, spatial normalization and smoothing of 8 mm). Then, the BOLD signal timecourse at each voxel was detrended and filtered (0.01 – 0.08 Hz). Using Marsbar toolbox in SPM (http://marsbar.sourceforge.net/), spurious signal variations were removed by regressing out the signals of lateral ventricles and the deep cerebral white matter. After preprocessing, functional data was co-registered to the structural T1-weighted scan of the subject. Then at the location of each iEEG electrode (see below), the BOLD signals of adjacent voxels within a 5mm radius was averaged to generate the region of interest (ROI) BOLD signal corresponding to that iEEG electrode (Similar to (Kucyi et al., 2018)). To minimize spatial overlap of fMRI ROIs, adjacent ROIs with less than 9mm distance were excluded from the functional connectomes of both iEEG and fMRI.

T1-space position of iEEG electrodes of each subject were estimated once the post-implantation CT scan of each subject was co-registered to their structural T1-weighted scan (Ridley et al., 2017). Then, the MNI location of the electrodes in each subject was calculated (shown in Fig. 1). Intracranial EEG data was corrected for gradient and cardio-ballistic artifacts using Brain Vision Analyzer software (Allen et al., 2000) and down-sampled to 250Hz. Proceeding a spike detection analysis (Bettus et al., 2011; Ridley et al., 2017), electrodes that were marked by clinicians as involved in generating seizures or generating interictal spikes were excluded

bioRxiv preprint doi: https://doi.org/10.1101/2022.06.17.496647; this version posted June 20, 2022. The copyright holder for this preprint (which was not certified by peer review) is the author/funder, who has granted bioRxiv a license to display the preprint in perpetuity. It is made available under aCC-BY-NC-ND 4.0 International license.

from further analyses. To remove slow drifts, line noise, and high-frequency noise, the data was filtered with a 4th-order high-pass Butterworth filter at 0.5 Hz, a 6th-order notch filter at 50Hz, and a 4th-order low-pass Butterworth filter at 90 Hz, respectively. Since interpretation of white matter BOLD signals is debated (Gawryluk et al., 2014), depth electrodes that were implanted in the white matter (and their corresponding fMRI ROIs) were excluded from the analyses. For this purpose, we excluded electrodes that were embedded outside of SPM's gray matter template mask in MNI space. Additionally, electrodes with remaining jump artifacts, highly prevalent periods of epileptiform activity, or low SNR were removed by visual inspections under supervision of an epileptologist. After this cleaning procedure, electrodes were re-referenced to the common average. Note that in order to preserve temporal continuity of the concurrent recordings, we did not exclude time intervals of the iEEG data that contained additional interictal activity in the healthy brain regions. However, to ensure that interictal activity had no critical effect on our findings, we generalized our observations in a non-clinical population (source-localized EEG-fMRI dataset) and further statistically demonstrated in the intracranial data the temporal independence of cross-modal similarity of connectome dynamics from visually marked epochs of interictal activity (19±15% of data length) (see last section of results).

Source-localized EEG-fMRI dataset: fMRI and EEG data were preprocessed with standard preprocessing steps as explained in details elsewhere (Wirsich et al., 2020b). In brief, fMRI underwent standard slice-time correction, spatial realignment (SPM12, http://www.fil.ion.ucl.ac.uk/spm/software/spm12). Structural T1-weighted images were processed using Freesurfer (recon-all, v6.0.0, https://surfer.nmr.mgh.harvard.edu/) in order to perform non-uniformity and intensity correction, skull stripping and gray/white matter segmentation. The cortex was parcellated into 68 regions of the Desikan-Kiliany atlas (Desikan et al., 2006). This atlas was chosen because —as an anatomical parcellation— avoids biases towards one or the other functional data modality. The T1 images of each subject and the Desikan atlas were co-registered to the fMRI images (FSL-FLIRT 6.0.2, https://fsl.fmrib.ox.ac.uk/fsl/fslwiki). We extracted signals of no interest such as the average signals of cerebrospinal fluid (CSF) and white matter from manually defined regions of interest (ROI, 5 mm sphere, Marsbar Toolbox 0.44, http://marsbar.sourceforge.net) and regressed out of the BOLD timeseries along with 6 rotation, translation motion parameters and global gray matter signal (Wirsich et al., 2017). Then we bandpass-filtered the timeseries at 0.009–0.08 Hz. Average timeseries of each region was then used to calculate connectivity.

EEG underwent gradient and cardio-ballistic artifact removal using Brain Vision Analyzer software (Allen et al., 1998, 2000) and was down-sampled to 250 Hz. EEG was projected into source space using the Tikhonov-regularized minimum norm in Brainstorm software (Baillet et al., 2001; Tadel et al., 2011). Band-limited source-reconstructed EEG signals in each canonical frequency band were then used to calculate frequency-specific connectome dynamics. Note that the MEG-ROI-nets toolbox in the OHBA Software Library (OSL; https://ohba-analysis.github.io/osl-docs/) was used to minimize source leakage (supplementary materials) in the band-limited source-localized EEG data (Colclough et al., 2015).

bioRxiv preprint doi: https://doi.org/10.1101/2022.06.17.496647; this version posted June 20, 2022. The copyright holder for this preprint (which was not certified by peer review) is the author/funder, who has granted bioRxiv a license to display the preprint in perpetuity. It is made available under aCC-BY-NC-ND 4.0 International license.

Connectivity analyses

Connectivity analyses were identical in the two datasets unless stated otherwise.

Dynamic measures of connectivity: Amplitude- and phase coupling (*EEG-FC$_{Amp}$ and EEG-FC$_{Phase}$*) are two measures of functional connectivity in neurophysiological data reflecting distinct coupling modes (Mostame and Sadaghiani, 2020b). In this study, we use both *EEG-FC$_{Amp}$* (for the main results) *and EEG-FC$_{Phase}$* (for replication purposes, see supplementary materials) and collectively refer to them as *iEEG FC* (or *EEG FC* for the source-localized scalp dataset). We investigate five canonical electrophysiological frequency bands: δ (1-4 Hz), θ (5-7 Hz), α (8-13 Hz), β (14-30 Hz), γ (31-60 Hz). To estimate iEEG/EEG FC at each canonical frequency band, we first band-passed the electrophysiological signals using a 4th-order Chebyshev type II filter. We used the Hilbert transform of the band-passed signals to extract the envelope and unwrapped phase of each signal.

Amplitude coupling (*EEG-FC$_{Amp}$*) was defined as the coupling of the z-scored activation amplitude of the two distinct electrodes, within the time window of FC estimation. Specifically, *EEG-FC$_{amp}$* between electrodes *i* and *j* at time *t* over the frequency band *freq* was calculated as:

$$EEG\_FC_{Amp}{}_{ij}^{freq}(t) = \frac{1}{N}\sum_{m=t-\frac{L}{2}}^{t+\frac{L}{2}} Z(env_i^{freq})(m) \times Z(env_j^{freq})(m)$$

where L is the window length (=4s), N is the number of data points within the window (specifically 1000 samples), and Z(env) is the envelope of the signal that is Z-scored with respect to its timepoints across the whole time of data acquisition. Note that our approach for estimating *EEG-FC$_{Amp}$* is a modified version of the fine-grained fMRI-FC measure recently introduced by Esfahlani and colleagues (2020). Given that iEEG signals are considerably faster than BOLD signals by nature, here the measure is averaged over N consecutive samples within a 4s window to increase SNR. The center of the window (timepoint *t)* stepped at every 100ms, providing an *EEG-FC$_{Amp}$* timecourse of 100ms resolution.

Major findings were replicated using an alternative mode of electrophysiology-derived connectivity, phase coupling (see supplementary materials). EEG-FC$_{Phase}$ was defined as the consistency of the phase difference of band-passed signals across an electrode pair, within the time window of length L (4s):

$$EEG\_FC_{Phase}{}_{ij}^{freq}(t) = \frac{1}{N}\sum_{m=t-\frac{L}{2}}^{t+\frac{L}{2}} e^{j\Delta\varphi_{ij}^{freq}(m)}$$

where $\Delta\varphi$ is the phase difference between the two signals.

bioRxiv preprint doi: https://doi.org/10.1101/2022.06.17.496647; this version posted June 20, 2022. The copyright holder for this preprint (which was not certified by peer review) is the author/funder, who has granted bioRxiv a license to display the preprint in perpetuity. It is made available under aCC-BY-NC-ND 4.0 International license.

The dynamic FC in fMRI data (fMRI-FC) was estimated using the original fine-grained measure of FC by Esfahlani and colleagues. *fMRI-FC* of ROIs *i* and *j* at time *t* was estimated as below, where Z(BOLD) is the Z-scored BOLD signal of the ROI with respect to its own timepoints.

$$fMRI\_FC_{ij}(t) = Z\big(BOLD_i(t)\big) \times Z\left(BOLD_j(t)\right)$$

We matched the temporal resolution of fMRI FC with iEEG FC by interpolating the dynamic FC of fMRI (from the respective TR to 100ms resolution) using the cubic spline method. Temporal up-sampling ensured that fMRI-FC, *EEG-FC$_{Amp}$, and EEG-FC$_{Phase}$* were at the same resolution (100ms), allowing us to directly compare the three measures, i.e. without degrading the temporal resolution of iEEG/EEG. Finally, to compensate for the time lag between hemodynamic and neural responses of the brain (Logothetis et al., 2001), we shifted the fMRI-FC timecourse 6 seconds backwards in time.

Static measures of connectivity: Static FC of each measure was extracted by averaging the connection-wise FC values across all timepoints of dynamic FC for *EEG-FC$_{Amp}$, EEG-FC$_{Phase}$,* and *fMRI-FC* respectively.

Statistical evaluation of cross-modal correlations: For each subject, we statistically assessed the significance of the cross-modal spatial similarity of connectome configurations -after compensating for the 6s hemodynamic lag- separately at each timepoint (synchronous approach) and at each pair of time-points (asynchronous approach), corrected for number of timepoints. To this end, we generated a set of randomized FC matrices by spatially phase-permuting the original iEEG and fMRI FC matrices – at the corresponding timepoint(s)- in 2D Fourier space and then reconstructing the matrices using the inverse 2D Fourier transform (Prichard and Theiler, 1994; Tewarie et al., 2016; Wirsich et al., 2017). A set of surrogate cross-modal spatial correlation values were estimated at each timepoint (or pair of timepoints for CRP analysis) using the described null data. Finally, at each timepoint (or pair of timepoints for CRP analysis), the original spatial correlation across fMRI and iEEG connectomes was compared to the estimated null distribution of spatial correlation values (100 randomizations). Multiple comparisons were corrected according to the number of timepoints (or pair of timepoints), using the Benjamini Hochberg FDR correction method ($q < 0.05$).

In the asynchronous analysis, the above-described approach resulted in one cross-modal CRP matrix per subject, EEG frequency band, and electrophysiological connectivity mode (EEG-FC$_{Amp}$ and EEG-FC$_{Phase}$). The frequency band-specific CRPs for each connectivity mode were overlaid into multi-frequency CRPs. At the level of individual subjects, the ratio between the significance rate of off- and on-diagonal CRP epochs (off-/on-diagonal ratio) entered a non-parametric test against a null distribution of chance-level off-/on-diagonal ratios. The null distribution was extracted from spatially phase-randomizing the multi-frequency CRPs in the 2D Fourier space and then reconstructing the matrices using the inverse 2D Fourier transform (100 randomizations). We additionally performed a Bayesian test to provide direct statistical evidence in favor of H0 (i.e. cross-modal temporal divergence; off-/on-diagonal ratio≈1) against H1 (i.e. temporal convergence; off-

bioRxiv preprint doi: https://doi.org/10.1101/2022.06.17.496647; this version posted June 20, 2022. The copyright holder for this preprint (which was not certified by peer review) is the author/funder, who has granted bioRxiv a license to display the preprint in perpetuity. It is made available under aCC-BY-NC-ND 4.0 International license.

/on-diagonal ratio<1). This statistical test was conducted in JASP software (https://jasp-stats.org/), using the default settings for the prior distribution (Cauchy distribution with scale parameter of 0.707).

Assessing inter-band temporal overlap of cross-modal co-occurrences: To find out whether the cross-modal similarities of fMRI and iEEG/EEG connectome dynamics are governed by a multi-frequency link, we employed an inter-band comparison in both synchronous and asynchronous analysis. For the synchronous analysis we quantified the temporal correlation of the frequency-specific similarity timecourses (color-coded timecourses in Fig. 2B) in a pairwise manner. Similarly, in the asynchronous analysis, we quantified the extent of inter-band temporal overlap of the significant CRP epochs (colored dots in the multi-frequency CRP in Fig. 3A) using the Jaccard index:

$$Jaccard(A,B) = \frac{\sum(A \,\&\, B)}{\sum(A \mid B)}$$

Where A and B are 2D CRP matrices with the same size, and *&* and | are logical "And" and "Or", respectively. Note that Jaccard index ranges between 0 (for completely non-overlapping vectors) to 1 (for completely matching vectors).

Clustering of discrete states and their cross-modal match: This analysis was performed in the source-localized EEG-fMRI dataset only, allowing us to investigate whole-brain connectome states that are shared across subjects. Separately for the CRP of each frequency band, we pooled all the fMRI and EEG connectome configurations corresponding to the significant CRP epochs across all subjects. Using K-means clustering, we extracted modality-specific group-level connectome *states* that give rise to the cross-modal spatial convergence in every frequency-specific CRP. We determined the optimal number of clusters using the Calinski Harabasz index (Caliński and Harabasz, 1974). *Within* each modality and for the (pooled) CRP of every frequency band, we assessed whether the connectome states were distinct from one another. To this end, we quantified pairwise spatial correlation of every pair of connectome states in a particular modality and compared it to correlations in a null model comprised of pseudo-states. Pseudo-states were generated from Monte-Carlo permutations of the two corresponding cluster labels (5000 repetitions; q<0.05; Benjamini Hochberg FDR-corrected for the number of state pairs). *Across* modalities and in the (pooled) CRP of every frequency band, we quantified the prevalence of significant entries at which a given fMRI-FC state paired with each EEG-FC state using the Jaccard index. The outcome was compared to a null model generated by randomly permuted cluster labels (5000 repetitions; q< 0.05, Benjamini Hochberg FDR-corrected for the number of state pairs). For each fMRI-FC state, the best matching EEG state was determined as the one with the highest z-score, i.e. most significant prevalence of pairing compared to the null.

Assessment of potential contribution from artifacts and other sources: To show that the observed cross-modal spatial convergence is not associated with major confounding factors, we quantified in each subject and dataset the temporal correlation between the cross-modal spatial similarity timecourse and the timecourses of overall

bioRxiv preprint doi: https://doi.org/10.1101/2022.06.17.496647; this version posted June 20, 2022. The copyright holder for this preprint (which was not certified by peer review) is the author/funder, who has granted bioRxiv a license to display the preprint in perpetuity. It is made available under aCC-BY-NC-ND 4.0 International license.

FC strength, head motion, and static connectome "prominence". This latter timecourse was calculated as the correlation between frame-by-frame connectome configurations in iEEG or fMRI to the static (i.e. time-averaged) connectome of that modality. The FC strength timecourse was quantified as the root sum squares of the frame-by-frame FC value over all connections of either fMRI or EEG. The head motion timecourse was measured as framewise displacement (FD) (Power et al., 2012). We compared the estimated temporal correlation values to corresponding null distributions of correlations generated by phase-permuting the cross-modal spatial similarity timecourse in the Fourier space (see subplots A-C in Fig. S7; group-level *t*-test against subject-specific mean values of 500 surrogate samples). Further, we quantified temporal overlap of the binary timecourse of intervals of visually marked epileptiform activity and the binarized (significance-thresholded) timecourse of cross-modal spatial similarity using the Jaccard index. We compared the outcome to a corresponding null distribution extracted from a temporally-shifted (by a random number of samples between 1 and the length of the original timecourse) version of the binarized cross-modal spatial similarity timecourse (see subplots D in Fig. S7; group-level *t*-test against subject-specific mean values of 500 surrogate samples). Finally, we replicated our major findings in the scalp data using source-orthogonalized signals to show that our findings are largely independent of source leakage (supplementary materials). Particularly, this approach removes any zero-lag temporal correlation between every pair of electrode signals using a multi-variate orthogonalization process so that any spurious correlation due to volume conduction would be minimized (Colclough et al., 2015).

References

Abreu R, Simões M, Castelo-Branco M (2020) Pushing the Limits of EEG: Estimation of Large-Scale Functional Brain Networks and Their Dynamics Validated by Simultaneous fMRI. Front Neurosci 14 Available at: https://www.frontiersin.org/articles/10.3389/fnins.2020.00323/full [Accessed June 28, 2021].

Allen PJ, Josephs O, Turner R (2000) A Method for Removing Imaging Artifact from Continuous EEG Recorded during Functional MRI. NeuroImage 12:230–239.

Allen PJ, Polizzi G, Krakow K, Fish DR, Lemieux L (1998) Identification of EEG Events in the MR Scanner: The Problem of Pulse Artifact and a Method for Its Subtraction. NeuroImage 8:229–239.

Baillet S, Mosher JC, Leahy RM (2001) Electromagnetic brain mapping. IEEE Signal Process Mag 18:14–30.

Baker AP, Brookes MJ, Rezek IA, Smith SM, Behrens T, Probert Smith PJ, Woolrich M (2014) Fast transient networks in spontaneous human brain activity Culham JC, ed. eLife 3:e01867.

Bettus G, Ranjeva J-P, Wendling F, Bénar CG, Confort-Gouny S, Régis J, Chauvel P, Cozzone PJ, Lemieux L, Bartolomei F, Guye M (2011) Interictal Functional Connectivity of Human Epileptic Networks Assessed by Intracerebral EEG and BOLD Signal Fluctuations. PLOS ONE 6:e20071.

Betzel RF, Medaglia JD, Kahn AE, Soffer J, Schonhaut DR, Bassett DS (2019) Structural, geometric and genetic factors predict interregional brain connectivity patterns probed by electrocorticography. Nat Biomed Eng:1.

bioRxiv preprint doi: https://doi.org/10.1101/2022.06.17.496647; this version posted June 20, 2022. The copyright holder for this preprint (which was not certified by peer review) is the author/funder, who has granted bioRxiv a license to display the preprint in perpetuity. It is made available under aCC-BY-NC-ND 4.0 International license.

Brookes MJ, Woolrich M, Luckhoo H, Price D, Hale JR, Stephenson MC, Barnes GR, Smith SM, Morris PG (2011) Investigating the electrophysiological basis of resting state networks using magnetoencephalography. Proc Natl Acad Sci 108:16783–16788.

Buzsáki G, Anastassiou CA, Koch C (2012) The origin of extracellular fields and currents — EEG, ECoG, LFP and spikes. Nat Rev Neurosci 13:407–420.

Cabral J, Kringelbach ML, Deco G (2017) Functional connectivity dynamically evolves on multiple time-scales over a static structural connectome: Models and mechanisms. NeuroImage 160:84–96.

Cabral J, Luckhoo H, Woolrich M, Joensson M, Mohseni H, Baker A, Kringelbach ML, Deco G (2014) Exploring mechanisms of spontaneous functional connectivity in MEG: How delayed network interactions lead to structured amplitude envelopes of band-pass filtered oscillations. NeuroImage 90:423–435.

Calhoun VD, Miller R, Pearlson G, Adalı T (2014) The Chronnectome: Time-Varying Connectivity Networks as the Next Frontier in fMRI Data Discovery. Neuron 84:262–274.

Caliński T, Harabasz J (1974) A dendrite method for cluster analysis. Commun Stat 3:1–27.

Chang C, Glover GH (2010) Time–frequency dynamics of resting-state brain connectivity measured with fMRI. NeuroImage 50:81–98.

Cohen JR (2018) The behavioral and cognitive relevance of time-varying, dynamic changes in functional connectivity. NeuroImage 180:515–525.

Colclough GL, Brookes MJ, Smith SM, Woolrich MW (2015) A symmetric multivariate leakage correction for MEG connectomes. Neuroimage 117:439–448.

Deco G, Jirsa V, McIntosh AR, Sporns O, Kötter R (2009) Key role of coupling, delay, and noise in resting brain fluctuations. Proc Natl Acad Sci 106:10302–10307.

Deco G, Jirsa VK, McIntosh AR (2013) Resting brains never rest: computational insights into potential cognitive architectures. Trends Neurosci 36:268–274.

Deligianni F, Carmichael DW, Zhang GH, Clark CA, Clayden JD (2016) NODDI and tensor-based microstructural indices as predictors of functional connectivity. PloS One 11:e0153404.

Deligianni F, Centeno M, Carmichael DW, Clayden JD (2014) Relating resting-state fMRI and EEG whole-brain connectomes across frequency bands. Front Neurosci 8:258.

Desikan RS, Ségonne F, Fischl B, Quinn BT, Dickerson BC, Blacker D, Buckner RL, Dale AM, Maguire RP, Hyman BT, Albert MS, Killiany RJ (2006) An automated labeling system for subdividing the human cerebral cortex on MRI scans into gyral based regions of interest. NeuroImage 31:968–980.

Dubey A, Ray S (2019) Cortical Electrocorticogram (ECoG) Is a Local Signal. J Neurosci 39:4299–4311.

Esfahlani FZ, Jo Y, Faskowitz J, Byrge L, Kennedy DP, Sporns O, Betzel RF (2020) High-amplitude cofluctuations in cortical activity drive functional connectivity. Proc Natl Acad Sci 117:28393–28401.

Gawryluk JR, Mazerolle EL, D'Arcy RCN (2014) Does functional MRI detect activation in white matter? A review of emerging evidence, issues, and future directions. Front Neurosci 8:239.

Gratton C, Laumann TO, Nielsen AN, Greene DJ, Gordon EM, Gilmore AW, Nelson SM, Coalson RS, Snyder AZ, Schlaggar BL, Dosenbach NUF, Petersen SE (2018) Functional Brain Networks Are Dominated by Stable Group and Individual Factors, Not Cognitive or Daily Variation. Neuron 98:439-452.e5.

bioRxiv preprint doi: https://doi.org/10.1101/2022.06.17.496647; this version posted June 20, 2022. The copyright holder for this preprint (which was not certified by peer review) is the author/funder, who has granted bioRxiv a license to display the preprint in perpetuity. It is made available under aCC-BY-NC-ND 4.0 International license.

Hari R, Parkkonen L (2015) The brain timewise: how timing shapes and supports brain function. Philos Trans R Soc B Biol Sci 370:20140170.

Heeger DJ, Ress D (2002) What does fMRI tell us about neuronal activity? Nat Rev Neurosci 3:142–151.

Hermes D, Nguyen M, Winawer J (2017) Neuronal synchrony and the relation between the blood-oxygen-level dependent response and the local field potential. PLOS Biol 15:e2001461.

Hipp JF, Siegel M (2015) BOLD fMRI correlation reflects frequency-specific neuronal correlation. Curr Biol 25:1368–1374.

Hunyadi B, Woolrich MW, Quinn AJ, Vidaurre D, De Vos M (2019) A dynamic system of brain networks revealed by fast transient EEG fluctuations and their fMRI correlates. NeuroImage 185:72–82.

Kucyi A, Schrouff J, Bickel S, Foster BL, Shine JM, Parvizi J (2018) Intracranial Electrophysiology Reveals Reproducible Intrinsic Functional Connectivity within Human Brain Networks. J Neurosci 38:4230–4242.

Logothetis NK, Pauls J, Augath M, Trinath T, Oeltermann A (2001) Neurophysiological investigation of the basis of the fMRI signal. Nature 412:150–157.

Lurie D et al. (2018) On the nature of resting fMRI and time-varying functional connectivity.

Mele G, Cavaliere C, Alfano V, Orsini M, Salvatore M, Aiello M (2019) Simultaneous EEG-fMRI for Functional Neurological Assessment. Front Neurol 10 Available at: https://www.frontiersin.org/article/10.3389/fneur.2019.00848 [Accessed January 28, 2022].

Mostame P, Sadaghiani S (2020a) Oscillation-Based Connectivity Architecture Is Dominated by an Intrinsic Spatial Organization, Not Cognitive State or Frequency. J Neurosci Available at: https://www.jneurosci.org/content/early/2020/11/16/JNEUROSCI.2155-20.2020 [Accessed December 10, 2020].

Mostame P, Sadaghiani S (2020b) Phase- and amplitude-coupling are tied by an intrinsic spatial organization but show divergent stimulus-related changes. NeuroImage 219:117051.

Mukamel R, Gelbard H, Arieli A, Hasson U, Fried I, Malach R (2005) Coupling Between Neuronal Firing, Field Potentials, and fMRI in Human Auditory Cortex. Science 309:951–954.

Mullinger K, Bowtell R (2011) Combining EEG and fMRI. In: Magnetic Resonance Neuroimaging: Methods and Protocols (Modo M, Bulte JWM, eds), pp 303–326 Methods in Molecular Biology. Totowa, NJ: Humana Press. Available at: https://doi.org/10.1007/978-1-61737-992-5_15 [Accessed January 28, 2022].

Nir Y, Fisch L, Mukamel R, Gelbard-Sagiv H, Arieli A, Fried I, Malach R (2007) Coupling between Neuronal Firing Rate, Gamma LFP, and BOLD fMRI Is Related to Interneuronal Correlations. Curr Biol 17:1275–1285.

Nunez PL, Silberstein RB (2000) On the relationship of synaptic activity to macroscopic measurements: does co-registration of EEG with fMRI make sense? Brain Topogr 13:79–96.

Power JD, Barnes KA, Snyder AZ, Schlaggar BL, Petersen SE (2012) Spurious but systematic correlations in functional connectivity MRI networks arise from subject motion. Neuroimage 59:2142–2154.

Preti MG, Bolton TA, Van De Ville D (2017) The dynamic functional connectome: State-of-the-art and perspectives. NeuroImage 160:41–54.

Prichard D, Theiler J (1994) Generating surrogate data for time series with several simultaneously measured variables. Phys Rev Lett 73:951–954.

bioRxiv preprint doi: https://doi.org/10.1101/2022.06.17.496647; this version posted June 20, 2022. The copyright holder for this preprint (which was not certified by peer review) is the author/funder, who has granted bioRxiv a license to display the preprint in perpetuity. It is made available under aCC-BY-NC-ND 4.0 International license.

Rabuffo G, Fousek J, Bernard C, Jirsa V (2021) Neuronal Cascades Shape Whole-Brain Functional Dynamics at Rest. eNeuro 8 Available at: https://www.eneuro.org/content/8/5/ENEURO.0283-21.2021 [Accessed May 8, 2022].

Rassi E, Wutz A, Müller-Voggel N, Weisz N (2019) Prestimulus feedback connectivity biases the content of visual experiences. Proc Natl Acad Sci 116:16056–16061.

Ridley B, Wirsich J, Bettus G, Rodionov R, Murta T, Chaudhary U, Carmichael D, Thornton R, Vulliemoz S, McEvoy A, Wendling F, Bartolomei F, Ranjeva J-P, Lemieux L, Guye M (2017) Simultaneous Intracranial EEG-fMRI Shows Inter-Modality Correlation in Time-Resolved Connectivity Within Normal Areas but Not Within Epileptic Regions. Brain Topogr 30:639–655.

Rouse AG, Williams JJ, Wheeler JJ, Moran DW (2016) Spatial co-adaptation of cortical control columns in a micro-ECoG brain–computer interface. J Neural Eng 13:056018.

Sadaghiani S, Brookes MJ, Baillet S (2021) Connectomics of Human Electrophysiology. Available at: https://psyarxiv.com/dr7zh/ [Accessed June 13, 2021].

Sadaghiani S, Brookes MJ, Baillet S (2022) Connectomics of human electrophysiology. NeuroImage 247:118788.

Sadaghiani S, D'Esposito M (2015) Functional Characterization of the Cingulo-Opercular Network in the Maintenance of Tonic Alertness. Cereb Cortex 25:2763–2773.

Sadaghiani S, Scheeringa R, Lehongre K, Morillon B, Giraud A-L, Kleinschmidt A (2010) Intrinsic Connectivity Networks, Alpha Oscillations, and Tonic Alertness: A Simultaneous Electroencephalography/Functional Magnetic Resonance Imaging Study. J Neurosci 30:10243–10250.

Sadaghiani S, Wirsich J (2019) Intrinsic connectome organization across temporal scales: New insights from cross-modal approaches. Netw Neurosci:1–49.

Tadel F, Baillet S, Mosher JC, Pantazis D, Leahy RM (2011) Brainstorm: A User-Friendly Application for MEG/EEG Analysis. Comput Intell Neurosci Available at: https://www.hindawi.com/journals/cin/2011/879716/ [Accessed December 1, 2019].

Tewarie P, Bright MG, Hillebrand A, Robson SE, Gascoyne LE, Morris PG, Meier J, Van Mieghem P, Brookes MJ (2016) Predicting haemodynamic networks using electrophysiology: The role of non-linear and cross-frequency interactions. Neuroimage 130:273–292.

Vohryzek J, Deco G, Cessac B, Kringelbach ML, Cabral J (2020) Ghost Attractors in Spontaneous Brain Activity: Recurrent Excursions Into Functionally-Relevant BOLD Phase-Locking States. Front Syst Neurosci 14 Available at: https://www.frontiersin.org/articles/10.3389/fnsys.2020.00020/full?report=reader [Accessed December 10, 2020].

Weisz N, Wühle A, Monittola G, Demarchi G, Frey J, Popov T, Braun C (2014) Prestimulus oscillatory power and connectivity patterns predispose conscious somatosensory perception. Proc Natl Acad Sci 111:E417–E425.

Wirsich J, Amico E, Giraud A-L, Goñi J, Sadaghiani S (2020a) Multi-timescale hybrid components of the functional brain connectome: A bimodal EEG-fMRI decomposition. Netw Neurosci 4:658–677.

Wirsich J, Giraud A-L, Sadaghiani S (2020b) Concurrent EEG- and fMRI-derived functional connectomes exhibit linked dynamics. NeuroImage 219:116998.

Wirsich J, Jorge J, Iannotti G, Shamshiri EA, Grouiller F, Abreu R, Lazeyras F, Giraud A-L, Gruetter R, Sadaghiani S, Vulliémoz S (2021) The relationship between EEG and fMRI connectomes is reproducible across simultaneous EEG-fMRI studies from 1.5T to 7T. NeuroImage:117864.

bioRxiv preprint doi: https://doi.org/10.1101/2022.06.17.496647; this version posted June 20, 2022. The copyright holder for this preprint (which was not certified by peer review) is the author/funder, who has granted bioRxiv a license to display the preprint in perpetuity. It is made available under aCC-BY-NC-ND 4.0 International license.

Wirsich J, Ridley B, Besson P, Jirsa V, Bénar C, Ranjeva J-P, Guye M (2017) Complementary contributions of concurrent EEG and fMRI connectivity for predicting structural connectivity. NeuroImage 161:251–260.

Yeo BT, Krienen FM, Sepulcre J, Sabuncu MR, Lashkari D, Hollinshead M, Roffman JL, Smoller JW, Zöllei L, Polimeni JR, Fischl B, Liu H, Buckner RL (2011) The organization of the human cerebral cortex estimated by intrinsic functional connectivity. J Neurophysiol 106:1125–1165.

Zhang X, Pan W-J, Keilholz SD (2020) The relationship between BOLD and neural activity arises from temporally sparse events. NeuroImage 207:116390.